UHASSELT
KNOWLEDGE IN ACTION

Maastricht University

Faculteit Geneeskunde en Levenswetenschappen
School voor Levenswetenschappen

master in de biomedische wetenschappen

Masterthesis

High-molecular-weight advanced glycation end products disturb the vasomotor balance in rat aortic rings through superoxide formation

Sibren Haesen

Scriptie ingediend tot het behalen van de graad van master in de biomedische wetenschappen, afstudeerrichting klinische moleculaire wetenschappen

PROMOTOR :
Prof. dr. Virginie BITO

COPROMOTOR :
dr. Dorien DELUYKER

2018
2019

De transnationale Universiteit Limburg is een uniek samenwerkingsverband van twee universiteiten in twee landen: de Universiteit Hasselt en Maastricht University.

UHASSELT
KNOWLEDGE IN ACTION

www.uhasselt.be
Universiteit Hasselt
Campus Hasselt:
Martelarenlaan 42 | 3500 Hasselt
Campus Diepenbeek:
Agoralaan Gebouw D | 3590 Diepenbeek

Faculteit Geneeskunde en Levenswetenschappen

School voor Levenswetenschappen

master in de biomedische wetenschappen

Masterthesis

High-molecular-weight advanced glycation end products disturb the vasomotor balance in rat aortic rings through superoxide formation

Sibren Haesen

Scriptie ingediend tot het behalen van de graad van master in de biomedische wetenschappen, afstudeerrichting klinische moleculaire wetenschappen

PROMOTOR :
Prof. dr. Virginie BITO

COPROMOTOR :
dr. Dorien DELUYKER

Table of contents

Acknowledgements

My 5-years education in Biomedical Sciences at Hasselt University comes to its end by finishing this master's thesis. It was a real pleasure to study at this University. In this section, I take the opportunity to express my gratitude to the people who have supported me, each of them in their own way.

In the first place, I would like to thank Dorien, or should I say doctor Deluyker ;)? As the term implies, you are truly a 'daily supervisor', in the sense that you were always there for me in the lab at any time. It would require a whole thesis to express my thanks to you, but I will try to summarize it in a few sentences. Dorien, I am grateful for your advice and support during practical work. By being an excellent teacher, you were very important in my early scientific career. But most of all, you believed in me right from the start. Therefore, it was a pleasure doing this internship under your supervision!

Furthermore, I would like to thank my principal supervisor prof. dr. Virginie Bito for welcoming me into the Cardiology group and for the opportunity to be involved in this project. Virginie, I will never forget our meetings at the coffee machine when you asked: 'Hoe gaat het?', in excellent Dutch by the way! Your enthusiasm and interest in what I was doing have strengthened my passion for cardiovascular research, for which I am incredibly grateful.

Another person who played an important role during my internship is Umare. Umare, thanks for your practical assistance as part of your junior internship. Without your outstanding efforts, the aorta experiments would never be possible.

Next, I would like to thank the Cardiology group: Maxim, Lize, and Hanne. To all of you, many thanks for your advice and help with the injections. In addition, I would like to thank the Physiology group for their feedback on experiments, Petra for her skillful technical assistance during the aorta experiments and dr. Ronald Driesen for his help during the morphological analysis of cardiomyocytes.

Another word of appreciation goes to prof. dr. Bert Op 't Eijnde, my second examiner, for his time to discuss the progression of my project. I appreciate your valuable feedback and suggestions that certainly improved this thesis, as well as your advice about my other research activities.

I would also like to thank all my fellow senior students for the good 'ambiance' during the internship period. There was a good mix of work and after-work activities with delicious lunch breaks. I wish you all the best in the future and I am sure that we will meet again somewhere!

Finally, I would like to thank the people who mean most to me. To my parents, brother, family, Ludo and Enza, I am very thankful for your immense support, for believing in me and for making sure I could find rest in between my schoolwork. However, my biggest thanks go to my girlfriend. Sarah, your enormous support has encouraged me to keep on going, but more importantly, has reminded me what matters most in life. I know that you will always stand by my side whatever happens, and that is more valuable than anything else.

List of abbreviations

ACh	Acetylcholine
AGEs	Advanced glycation end products
ALT-711	Alagebrium
ANOVA	Analysis of variance
ATP	Adenosine triphosphate
BH_4	Tetrahydrobiopterin
BSA	Bovine serum albumin
cGMP	Cyclic guanosine monophosphate
CML	N-carboxymethyllysine
COX	Cyclooxygenase
DAG	Diacylglycerol
DMSO	Dimethyl sulfoxide
EC_{50}	Half-maximal effective concentration
EDP	End-diastolic pressure
EDTA	Ethylenediaminetetraacetic acid
ELISA	Enzyme-linked immunosorbent assay
EM	Electron microscopy
E_{max}	Maximal relaxation
eNOS	Endothelial nitric oxide synthase
ET-1	Endothelin 1
HMW-AGEs	High-molecular-weight advanced glycation end products
HR	Heart rate
HRP	Horseradish peroxidase
ICAM-1	Intercellular adhesion molecule 1
IL-1α	Interleukin 1 alfa
IL-6	Interleukin 6
INDO	Indomethacin
IP	Intraperitoneal
IP_3	Inositol trisphosphate
LM	Light microscopy
LMW-AGEs	Low-molecular-weight advanced glycation end products
L-NAME	N(ω)-nitro-L-arginine methyl ester
LOX	Lysyl oxidase
LV	Left ventricle
MAPK	Mitogen-activated protein kinase
Max dP/dt	Maximum peak time derivative

Min dP/dt	Minimum peak time derivative
mTOR	Mechanistic target of rapamycin
NADPH	Nicotinamide adenine dinucleotide phosphate
NF-κB	Nuclear factor kappa B
NO	Nitric oxide
PBS	Phosphate-buffered saline
PE	Phenylephrine
PGI_2	Prostacyclin
PI3K	Phosphoinositide 3-kinase
PIP_2	Phosphatidylinositol 4,5-bisphosphate
PKB	Protein kinase B
RAGE	Receptor for advanced glycation end products
ROS	Reactive oxygen species
SEM	Standard error of the mean
SERCA	Sarcoplasmic reticulum calcium ATPase
SNP	Sodium nitroprusside
SOD	Superoxide dismutase
sRAGE	Soluble RAGE
TNF-α	Tumor necrosis factor alfa
VCAM-1	Vascular cell adhesion molecule 1

Summary

Background: Advanced glycation end products (AGEs) are compounds formed by the irreversible glycation of proteins. Growing evidence supports their contribution to cardiovascular disease, the leading cause of death worldwide. Our group has recently demonstrated that high-molecular-weight AGEs (HMW-AGEs) impair cardiac function in healthy rats. Preliminary data indicate that this adverse cardiac phenotype is related to altered functional properties of cardiomyocytes. However, the exact mechanism by which HMW-AGEs mediate these adverse cellular changes and the effect of HMW-AGEs on vascular function remain unclear. Therefore, the aim of this project is to 1) examine the effect of HMW-AGEs on vascular function and 2) investigate whether previously observed cardiac dysfunction is due to ultrastructural abnormalities in cardiomyocytes.

Materials and methods: Male Sprague Dawley rats were randomly assigned to daily intraperitoneal (IP) injection with either HMW-AGEs (20 mg/kg/day, N=12) or an equal volume of control solution (5.5 mg/kg/day, N=12) for six weeks. At week 6, plasma AGEs levels were quantified and left ventricular (LV) hemodynamic measurements were performed. After sacrifice, aortae were isolated. Vascular relaxation in response to cumulative doses of acetylcholine (ACh, 10^{-10}-10^{-5} M) or sodium nitroprusside (SNP, 10^{-10}-10^{-6} M) was evaluated in rat aortic rings precontracted with phenylephrine (PE, 10^{-7} M). Relaxation responses to ACh were also assessed in the presence of N(ω)-nitro-L-arginine methyl ester (L-NAME, 10^{-4} M), superoxide dismutase (SOD, 150 kU) or indomethacin (INDO, 10^{-5} M). LV tissue was processed for light microscopic (LM) examination of the mitochondrial area in cardiomyocytes. Finally, morphometric analysis of ultrastructural cardiomyocyte organization was performed with electron microscopy (EM). Statistical analysis was performed by t-test or two-way ANOVA corrected for multiple comparisons.

Results: HMW-AGEs injections in rats significantly increased circulating AGEs levels. Moreover, HMW-AGEs animals displayed cardiac dysfunction characterized by a significant increase in LV pressure. In addition, HMW-AGEs enhanced aortic contraction in response to a single dose of PE. The vasorelaxation response to ACh but not to SNP was significantly impaired in HMW-AGEs animals, as shown by reduced maximal relaxation (E_{max}) and a trend towards higher dose necessary to obtain half-maximal response (EC_{50}). SOD fully restored relaxation in aortic rings from HMW-AGEs animals, as demonstrated by increased E_{max} and reduced EC_{50} values. Relaxation of aortic rings from HMW-AGEs and control animals was blocked by L-NAME, yet the extent of inhibition was not different between both groups. The inhibitory effect of INDO was less pronounced in HMW-AGEs animals. Finally, HMW-AGEs increase cytoplasmic fraction and reduce mitochondrial area and number in cardiomyocytes.

Conclusion: Our data indicate that HMW-AGEs disturb the vasomotor balance in rat aortic rings through endothelial dysfunction and superoxide formation. In addition, we show that HMW-AGEs cause ultrastructural remodeling in cardiomyocytes. By elucidating the impact of HMW-AGEs on ultrastructural cardiomyocyte organization and demonstrating a direct link between HMW-AGEs and vascular dysfunction, we provide more insight into their role in cardiovascular disease. This research opens new opportunities for future experiments in the context of HMW-AGEs-induced cardiovascular dysfunction.

Keywords: advanced glycation end products – vasorelaxation – aorta – superoxide – mitochondria

Samenvatting

Achtergrond: Er is groeiend bewijs dat *advanced glycation end products (AGEs)* of versuikerde eiwitten bijdragen aan het ontstaan van cardiovasculaire aandoeningen, de voornaamste doodsoorzaak wereldwijd. Onze onderzoeksgroep heeft onlangs aangetoond dat AGEs met een hoog moleculair gewicht (HMW-AGEs) de hartfunctie verstoren in gezonde ratten. Voorlopige gegevens wijzen erop dat dit ongunstige cardiale fenotype gerelateerd is aan veranderde functionele eigenschappen van hartspiercellen. Het exacte mechanisme waarbij HMW-AGEs deze ongunstige cellulaire veranderingen mediëren blijft echter onduidelijk, net als hun effect op de vasculaire functie. Bijgevolg is het doel van dit project om 1) het effect van HMW-AGEs op vasculaire functie te onderzoeken en 2) na te gaan of ultrastructurele afwijkingen in hartspiercellen de eerder waargenomen hartdisfunctie veroorzaken.

Materiaal en methoden: Mannelijke ratten werden dagelijks intraperitoneaal (IP) geïnjecteerd met HMW-AGEs (20 mg/kg/dag, N=12) of een controle oplossing (5.5 mg/kg/dag, N=12) gedurende zes weken. Op het einde van week 6 werd de hoeveelheid AGEs in het bloed gemeten en werden hemodynamische metingen van de linkerventrikel (LV) uitgevoerd. Geïsoleerde aortaringen werden samengetrokken met een enkele dosis fenylefrine (PE, 10^{-7} M) voordat de vasculaire relaxatie als reactie op toenemende dosissen van acetylcholine (ACh, 10^{-10}-10^{-5} M) of natriumnitroprusside (SNP, 10^{-10}-10^{-6} M) werd gemeten. De relaxatierespons op ACh werd ook bepaald in aanwezigheid van N(ω)-nitro-L-arginine methyl ester (L-NAME, 10^{-4} M), superoxidedismutase (SOD, 150 kU) of indometacine (INDO, 10^{-5} M). De mitochondriale oppervlakte werd gemeten na lichtmicroscopisch (LM) onderzoek van LV-hartweefsel. Ten slotte werd de ultrastructurele organisatie van hartspiercellen beoordeeld met elektronenmicroscopie (EM). Statistische analyse werd uitgevoerd met een t-test of tweeweg ANOVA.

Resultaten: HMW-AGEs injecties in ratten verhoogden de circulerende AGEs concentraties. Daarnaast vertoonden HMW-AGEs dieren hartdisfunctie, gekarakteriseerd door een significante stijging van de drukken in het LV. HMW-AGEs versterkten ook de contractie van aortaringen als reactie op een enkele dosis PE. Bovendien was de relaxatierespons op ACh, maar niet op SNP, significant verzwakt in HMW-AGEs dieren zoals blijkt uit een verlaagde maximale relaxatie (E_{max}) en een trend richting een hogere dosis die nodig is om een half maximale reactie te induceren (EC_{50}). SOD herstelde de relaxatiecapaciteit in aortaringen van HMW-AGEs dieren, aangetoond door een verhoging van E_{max} en een verlaging van EC_{50} waarden. De relaxatie in aortaringen van HMW-AGEs en controle dieren werd geblokkeerd door L-NAME, maar de mate van remming was niet verschillend tussen beide groepen. Het inhiberende effect van INDO was minder uitgesproken in HMW-AGEs dieren. Ten slotte verhoogden HMW-AGEs de cytoplasmatische fractie in hartspiercellen en verminderden ze de mitochondriale oppervlakte net als het aantal mitochondriën.

Conclusie: Onze data tonen aan dat HMW-AGEs de vasomotor balans in rat aortaringen verstoren als gevolg van endotheeldisfunctie en superoxidevorming. Bovendien geven we aan dat HMW-AGEs zorgen voor de ultrastructurele vervorming van hartspiercellen. Hierbij bieden we meer inzicht in de rol van HMW-AGEs in cardiovasculaire aandoeningen en is dit project de aanzet voor toekomstig onderzoek in de context van cardiovasculaire disfunctie.

Trefwoorden: versuikerde eiwitten – vasculaire relaxatie – aorta – superoxide – mitochondriën

1 Introduction

1.1 Advanced glycation end products

In the early 1900s, the French scientist Louis Camille Maillard (1878-1936) incubated proteins in a glucose solution as part of his research on nutritional properties. After heat treatment, he observed a brownish pigment known today as advanced glycation end products (AGEs) (1). This 'browning' effect or advanced glycation involves a series of non-enzymatic reactions recognized as the Maillard reaction, a tribute to its founder. Later, it has been found that this reaction also occurs inside the human body during the normal aging process. However, the accumulation of AGEs accelerates in the presence of high glucose levels, as seen in diabetic patients (2). Since this discovery, the formation of AGEs and their impact on public health has been a major topic in cardiovascular research.

1.1.1 Formation of AGEs: the importance of heating and oxygen

AGEs is a collective term for the heterogeneous group of compounds formed by the irreversible glycation of proteins (3). In the initial step of the Maillard reaction, carbonyl groups of reducing sugars (*e.g.* glucose) react with amino groups of proteins to form unstable compounds known as Schiff bases (Figure 1) (4). This reaction is fast, reversible and depends on the availability of sugar substrates. The thermodynamically unfavored state forces Schiff bases to rearrange. This rearrangement is slower and yields more stable glycated proteins named Amadori products. Subsequent to Amadori rearrangement, structural modification (*e.g.* fragmentation and oxidation) of these products initiates the irreversible formation of AGEs (4). Especially oxidative modification is crucial in this last step as the rate of AGEs formation depends on the extent of oxidation. During increased oxidative stress, AGEs formation increases (5). In addition, AGEs enhance reactive oxygen species (ROS) production through their interaction with receptors, favoring their own production. Besides the direct contribution of aberrant oxidation to AGEs formation, AGEs also accumulate through autoxidation of glucose, lipids and proteins. This results in the production of carbonyl species (*i.e.* methylglyoxal, 3-deoxyglucosone and glycolaldehyde), the buildup of which refers to 'carbonyl stress' (Figure 1). Nowadays, these highly reactive carbonyl compounds, also formed during the degradation of Schiff bases and Amadori products, are recognized as key mediators in AGEs formation (6).

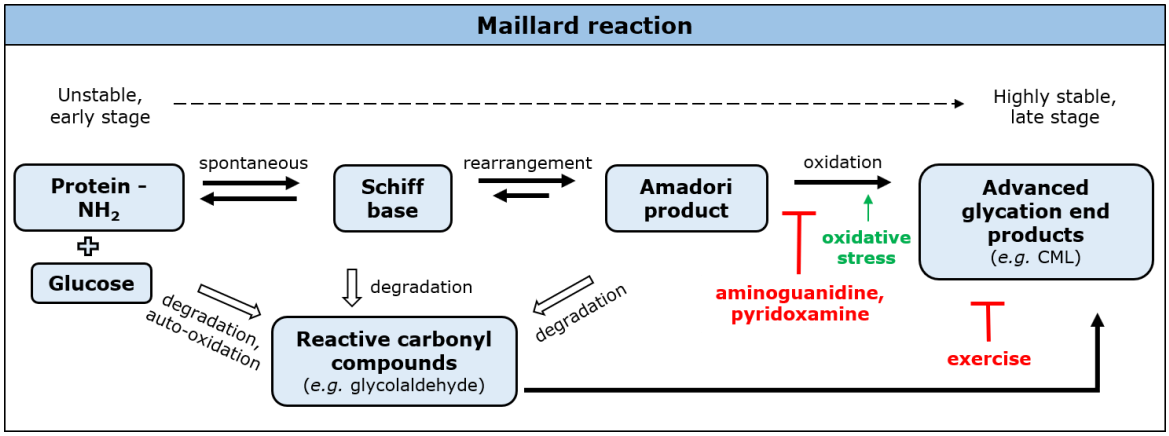

Figure 1: Internal formation of AGEs through the Maillard reaction. The interaction between proteins and sugars leads to spontaneous formation of Schiff bases, rearrangement to Amadori products, and irreversible formation of AGEs through oxidative modification. Oxidative stress stimulates AGEs formation, while aminoguanidine, pyridoxamine and exercise prevent this process. *CML = N-carboxymethyllysine.*

In addition to their internal formation, AGEs also derive from exogenous sources of which the modern Western diet stands out. The food industry currently uses AGEs to produce a pleasing flavor, color and texture of foods, of which fatty products (*e.g.* butter) and processed animal meat (*e.g.* beef) contain the highest AGEs content (7). The type of food distinguishes low- from high-AGEs diets (fats > proteins > carbohydrates), while the processing of food determines the rate of AGEs formation. Overall, a long cooking time combined with intense heating (*e.g.* frying, grilling or roasting) creates the highest AGEs content (7). The intestines absorb about 10% of food-derived AGEs, of which two-thirds enters the circulation via passive diffusion (free AGEs) or active transport (peptide-bound AGEs). The kidneys excrete the remaining one-third of the absorbed AGEs (8). The intake of a high-AGEs diet increases circulating AGEs levels and, consequently, predestines their accumulation in cardiovascular tissue (9). Besides food and food processing, tobacco smoke is another exogenous source of AGEs (10). This emphasizes that lifestyle and AGEs formation are inseparable in this era of fast food and cigarettes.

1.1.2 Classification of AGEs: more than just one compound

AGEs are very heterogeneous in both structure and function. Therefore, proper classification is essential to accurately detect these different entities. AGEs are usually categorized into three subgroups based on their autofluorescence properties and ability to form protein cross-links (11). The first subgroup consists of autofluorescent molecules that form protein cross-links in cardiovascular tissue, of which pentosidine is the typical example. The characteristic fluorescence pattern distinguishes this type of molecules from the second subgroup, the non-fluorescent cross-linking AGEs (*i.e.* imidazolium and glucosepane). The best-characterized AGEs compound, N-carboxymethyllysine (CML), belongs to the third subgroup or non-cross-linking AGEs (11).

AGEs can also be classified into low-molecular-weight (LMW-AGEs) and high-molecular-weight AGEs (HMW-AGEs) and detected accordingly by mass spectrometry (12). Low-molecular-weight AGEs (<12 kDa) are free proteins, while high-molecular-weight AGEs (>12 kDa) are protein-bound cross-linking compounds (13). Most researchers consider the level of LMW-AGEs, mainly CML, as a surrogate for total AGEs and correlate this class with the adverse cardiac phenotype. However, non-CML AGEs correlate better with the severity of microvascular complications in diabetic patients, suggesting a pivotal role for HMW-AGEs in this pathology (14). Moreover, Deluyker et al. (2016) have recently demonstrated that HMW-AGEs increase anterior and posterior wall thickness, typical signs of cardiac hypertrophy, and enhance the formation of cardiac fibrosis (15). Hence, distinguishing AGEs compounds according to their molecular weight is essential to understand their distinct role in cardiovascular diseases.

1.1.3 Actions of AGEs: cross-linking versus RAGE activation

In general, AGEs act by two mechanisms: damaging intra- and extracellular molecules or impairing cellular function after receptor activation (3). Firstly, AGEs alter the structural and mechanical properties of proteins by the process of cross-linking. Because AGEs formation takes multiple weeks, advanced glycation usually affects stable and long-lived proteins of the extracellular matrix (16). Especially collagen, the main structural component of connective tissue in the myocardium and vessel wall, is susceptible to glycation because of its slow turnover rate. Pathological cross-linking of AGEs with collagen fibrils renders them less distensible and more resistant to proteolytic breakdown.

In other words, normal tissue remodeling is impaired, which promotes stiffening of structurally inadequate fibrils in the myocardium and vessel wall (15, 17). AGEs modification of proteins naturally occurs during aging but accelerates with excessive blood glucose levels, as observed in diabetic patients (16). At the cardiomyocyte level, AGEs can cross-link intracellular proteins involved in the excitation-contraction coupling, including domains of the ryanodine receptor (18) and sarcoplasmic reticulum ATPase (SERCA) (19), leading to impaired calcium handling and altered cardiac relaxation.

The second way by which AGEs mediate their effects is through receptor activation. Several AGEs receptors have been described, of which the receptor for advanced glycation end products (RAGE) mediates most biological effects of AGEs (20). RAGE is a cell-surface receptor that belongs to the immunoglobulin superfamily. The receptor has three extracellular domains, a single transmembrane domain and a cytosolic tail that is essential to mediate intracellular signaling (21). Alternative splicing of the RAGE gene generates two isoforms next to the full-length RAGE receptor, named dominant-negative RAGE and soluble RAGE (sRAGE). Because they lack a cytosolic tail, these RAGE isoforms act as a decoy receptor by competitively binding AGEs, facilitating their removal instead of evoking intracellular signaling (21). RAGE is predominantly expressed in lung tissue, while cardiovascular tissue cells such as endothelial cells, vascular smooth muscle cells and cardiomyocytes express RAGE at a lower level. However, cardiac RAGE expression becomes upregulated with impaired heart function during aging and in pathological situations such as diabetes, myocardial infarction and ischemia-reperfusion (22). In this regard, stressed and damaged cells release AGEs ligands that interact with RAGE, thereby initiating key intracellular signaling pathways. These signaling cascades then trigger activation of the downstream effector nuclear factor kappa B (NF-κB), which induces the transcription of numerous adhesion molecules, growth factors, pro-coagulant factors and pro-inflammatory cytokines (23). However, Deluyker et al. (2016) have shown that HMW-AGEs neither alter RAGE expression nor change the expression of NF-κB inflammatory target genes including tumor necrosis factor alfa (TNF-α) and interleukin 6 (IL-6) (15). This indicates that activation of the RAGE-signaling pathway depends on the molecular weight of the AGEs compounds. A key consequence of AGEs-RAGE binding is the production of ROS by nicotinamide adenine dinucleotide phosphate (NADPH) oxidase, thereby increasing oxidative stress (24). Moreover, NF-κB upregulates the expression of RAGE itself, strengthening maintenance and amplification of the pro-inflammatory and pro-oxidant signal after RAGE activation (25).

1.2 The implication of AGEs in vascular dysfunction

The accumulation of AGEs leads to impaired vascular function by influencing large central arteries (*e.g.* aorta) both intra- and extracellularly (Figure 2). First, they directly cross-link extracellular collagen proteins thereby inducing vascular stiffening (16). Second, AGEs interact with RAGE expressed on cells implicated in vascular homeostasis, like platelets, immune cells, vascular smooth muscle cells and endothelial cells (22). Subsequently, AGEs indirectly affect endothelial function and vascular permeability through RAGE-mediated intracellular signaling (26). These vascular effects have been extensively described in diabetes, atherosclerosis and renal failure (3). In diabetic patients, serum AGEs levels inversely correlate with the extent of endothelial dysfunction measured by high-resolution ultrasound (27).

1.2.1 Receptor-independent effect: vascular stiffening

Stiffening of central elastic arteries such as the aorta is a characteristic physiological change during aging (28). However, this process accelerates in diabetic patients with high circulating AGEs levels, demonstrating a firm link between AGEs formation and vascular dysfunction (29). This link is of relevance because AGEs accumulate in the aortic vessel wall and increase collagen deposition between the endothelium and vascular smooth muscle, which contributes to aortic stiffening (26). Indeed, the degree of aortic stiffness positively correlates with AGEs tissue content, as shown by histological examination of human aortas (30). In addition, AGEs stimulate vascular smooth muscle cell proliferation and alter the activity of matrix metalloproteinases, further contributing to adverse tissue remodeling (31, 32). Aortic stiffening diminishes normal arterial elasticity and compliance. This clinically manifests as increased systolic blood pressure or isolated systolic hypertension. Accordingly, due to an increase in cardiac afterload, patients display left ventricular (LV) hypertrophy and delayed LV diastolic filling (33). Vascular compliance, as an indicator of arterial health, predicts the prognosis of the patient since reduced arterial compliance is associated with increased cardiovascular and all-cause mortality (33). This emphasizes the importance of anti-AGEs strategies to improve cardiovascular outcome, as will be explained later.

Besides their influence on vascular structure, AGEs also have direct effects on the main vascular function, that is regulating vasomotor tone (34). AGEs inactivate nitric oxide (NO), the most important vasorelaxant factor produced by endothelial cells. Pre-formed AGEs, as well as reactive intermediates such as methylglyoxal, quench NO, thereby reducing its bioavailability and activity (34). Furthermore, AGEs also interfere with NO formation mediated by endothelial NO synthase (eNOS). In concrete terms, culturing endothelial cells with AGEs downregulates eNOS expression through mRNA degradation and attenuates serine phosphorylation in this enzyme, eventually suppressing its activity (24).

1.2.2 Receptor-dependent effect: endothelial dysfunction

Pioneering work by the group of David M. Stern led to the identification of RAGE as a signal transduction receptor for AGEs in endothelial cells (20, 22). AGEs modulate endothelial cell properties through intracellular RAGE signaling. This implies disturbing the balanced secretion of relaxing and contracting factors that regulate vasomotor tone and perturbing endothelial barrier function (26). In this process, excessive generation of ROS plays a crucial role as endothelial RAGE signaling stimulates NADPH oxidase to generate superoxide, eventually reducing NO bioavailability (35). More specifically, superoxide radicals react with vascular NO to form peroxynitrite, a highly cytotoxic oxidant known to damage lipids through peroxidation (36). Peroxynitrite can oxidize and diminish the levels of tetrahydrobiopterin (BH_4), the cofactor essential for eNOS to produce NO, leading to a phenomenon referred to as 'eNOS uncoupling' (37). This state favors the synthesis of superoxide rather than NO, thus causing a vicious circle of NO depletion. In other words, the otherwise protective enzyme participating in the regulation of vasomotor tone turns into a ROS producer that contributes to AGEs-induced endothelial dysfunction (37). In addition, endothelial cells treated with increasing concentrations of AGEs produce less prostacyclin (PGI_2), another important vasorelaxant factor secreted by the endothelium, also via RAGE activation (38). AGEs-RAGE interaction on the endothelium and subsequent upregulation of NF-κB increases the expression of the vasoconstrictor endothelin 1 (ET-1), thereby stimulating vasocontraction in addition to impairing vasorelaxation (39).

Besides the inability to maintain normal vasomotor tone, endothelial dysfunction also manifests as a loss of barrier integrity by disrupting the vascular endothelial cadherin complex (40). The induction of vascular hyperpermeability is yet another RAGE-dependent effect of AGEs sustained by ROS production, facilitating monocyte adhesion to the endothelium and migration into the vascular intima. This results in a chronic inflammatory response and formation of foam cells, consequently promoting the development of atherosclerotic lesions (41).

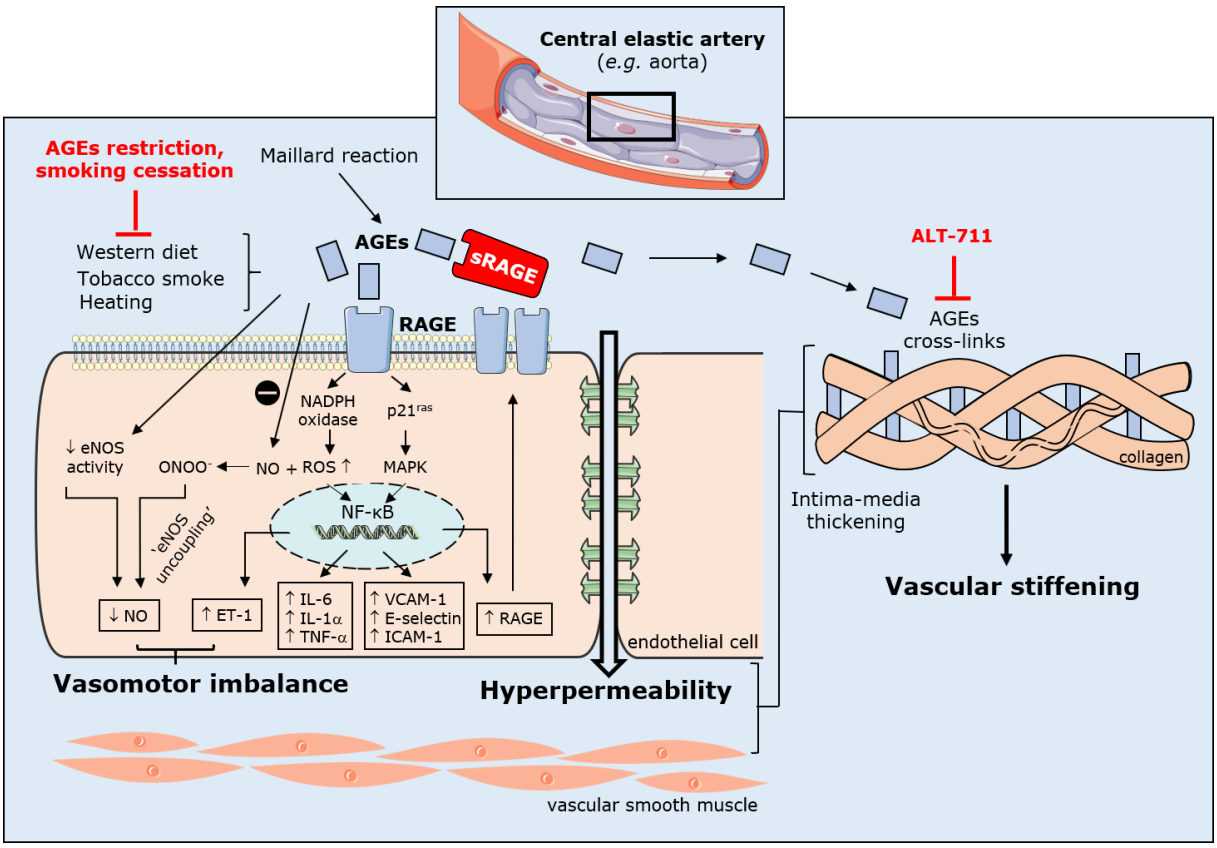

Figure 2: Intra- and extracellular effects of AGEs on vascular function and therapeutic targets. *Intracellular:* AGEs bind to endothelial RAGE, thereby inducing ROS production (*i.e.* superoxide) and activating intracellular signaling pathways. ROS accumulation inactivates NO and activates transcription factor NF-κB. Target genes include vasoconstrictors (*e.g.* ET-1), pro-inflammatory cytokines (*e.g.* TNF-α) and adhesion molecules (*e.g.* VCAM-1), leading to vasomotor imbalance and endothelial hyperpermeability. *Extracellular:* AGEs accumulate in the vessel wall, which results in increased collagen production, intima-media thickening and AGEs-collagen crosslinking, all of these effects contributing to vascular stiffening. AGEs also directly reduce eNOS activity and directly quench NO. Dietary AGEs restriction reduces AGEs intake, ALT-711 breaks pre-existing AGEs-protein cross-links and sRAGE acts as decoy receptor. *AGEs = advanced glycation end products, RAGE = receptor for advanced glycation end products, sRAGE = soluble RAGE, ALT-711 = alagebrium, MAPK = mitogen-activated protein kinase, NADPH oxidase = nicotinamide adenine dinucleotide phosphate oxidase, NO = nitric oxide, $ONOO^-$ = peroxynitrite, eNOS = endothelial NO synthase, ROS = reactive oxygen species, NF-κB = nuclear factor kappa-light-chain-enhancer of activated B cells, ET-1 = endothelin 1, IL-6 = interleukin 6, IL-1α = interleukin 1 alfa, VCAM-1 = vascular cell adhesion molecule 1, ICAM-1 = intercellular adhesion molecule 1.*

1.3 Anti-AGEs therapies to tackle vascular dysfunction

Bearing in mind the deleterious effects of AGEs on vascular function and their involvement in diverse cardiovascular pathologies, it is of great interest to interfere in this process (Figure 1 and 2). Therapeutic agents can be divided into 1) those that prevent AGEs-induced damage by inhibiting their formation and 2) those that address existing damage by breaking AGEs-protein cross-links or limiting RAGE activation (42). Furthermore, lifestyle modification can modulate AGEs intake from exogenous sources like heated food and cigarette smoke (9).

1.3.1 Inhibiting the formation of AGEs: prevent damage from happening

In the mid-1980s, Ulrich and Cerami proposed the concept of therapeutically inhibiting AGEs formation for the first time and evaluated the effect of the hydrazine compound aminoguanidine (43). Aminoguanidine is successful in preventing the formation of AGEs *in vitro* and its administration reverses diabetes-associated AGEs formation and collagen cross-linking in the aortic vessel wall (43). This is accompanied by improved arterial distensibility and reduced vascular stiffness (44). Moreover, aminoguanidine treatment prevents NO quenching by AGEs and thereby ameliorates impaired aortic relaxation in diabetic rats (34). Later, it was found that aminoguanidine mediates these positive effects by trapping highly reactive carbonyl intermediates of the Maillard reaction, hence preventing their conversion into mature AGEs compounds (45).

A second AGEs formation inhibitor is the vitamin B_6 derivative pyridoxamine. Pyridoxamine scavenges ROS, prevents the degradation of Amadori products to AGEs compounds, and neutralizes reactive carbonyl species. Indeed, pyridoxamine treatment reduces the levels of both AGEs precursors (*e.g.* methylglyoxal) and mature AGEs compounds (*e.g.* CML and pentosidine) (46). Moreover, pyridoxamine attenuates aortic and myocardial stiffening by inhibiting the formation of AGEs-mediated collagen cross-links (47, 48). Recently, Deluyker et al. (2017) have demonstrated that pyridoxamine, administered to rats via the drinking water, decreases circulating AGEs levels and thereby limits cardiovascular dysfunction after myocardial infarction. This positive outcome was due to a reduction of myocardial collagen content and lysyl oxidase (LOX) expression, a protein involved in collagen cross-linking (48).

1.3.2 Addressing the actions of AGEs: damage control

Alagebrium, also known as ALT-711, has the capacity to cleave existing cross-links thanks to its thiazolium structure. ALT-711 has been extensively tested as therapeutic for cardiovascular diseases in both preclinical- and clinical settings (49). In diabetic rats, ALT-711 treatment reversed diabetes-related large artery stiffness as demonstrated by increased systemic arterial compliance and collagen solubility, which is key to effective cross-link breaking (50). Vaitkevicius et al. (2001) have shown similar findings after examining the effect of ALT-711 on arterial and LV properties in aged nondiabetic rhesus monkeys (51). In parallel, clinical trials investigated vascular function in nondiabetic hypertensive patients after eight weeks of ALT-711 treatment (52, 53). Kass et al. (2001) have shown that ALT-711 improves arterial compliance in older individuals (>50 years) with age-dependent vascular stiffness (52). As shown by the same research group, ALT-711 also improved endothelial function, as reflected by increased flow-mediated dilation. Furthermore, flow-mediated dilation was negatively correlated with markers of vascular fibrosis and tissue remodeling (53).

Although ALT-711 yields favorable results on restoring vascular function in cardiovascular disease patients, evidence of its potential benefit to patient prognosis (*e.g.* survival rate) is lacking.

Another promising method to address the deleterious effects of AGEs is blocking their interaction with RAGE. As already mentioned, sRAGE acts as a decoy receptor for AGEs, thereby preventing RAGE activation and, accordingly, blocking intracellular signaling (21). The protective role of sRAGE has been tested widely in animal models of atherosclerosis (54, 55). For example, Park et al. (1998) have demonstrated a suppression of atherosclerosis development when diabetic mice developing spontaneous atherosclerosis were treated with exogenous sRAGE (54). Moreover, sRAGE stabilized the progression of the disease as shown by a reduction in the number and area of atherosclerotic lesions (55), illustrating preventive as well as therapeutic activity of sRAGE. In addition, administering sRAGE reverses the hypertension-related increase in aortic AGEs and collagen content, aortic hypertrophy, and impairment of aortic relaxation (56). At the molecular level, sRAGE treatment reduces NF-κB signaling, inflammation, tissue remodeling and oxidative stress in rat aortae (55, 56). In line with this observation, sRAGE reverses diabetes-induced vascular hyperpermeability in a dose-dependent manner (57). Despite these optimistic results in a preclinical setting, human trials on sRAGE intervention are necessary to translate this approach to clinical practice. Interestingly, endogenous sRAGE has recently been found as a predictor of endothelial dysfunction and a marker for cardiovascular disease and mortality risk (58).

1.3.3 Lifestyle modification: AGEs as modifiable risk factors

Non-pharmacologic options like dietary AGEs restriction, smoking cessation and exercise intervention, together known as a healthy lifestyle, are also efficient to reduce circulating AGEs levels (8, 10). Recently, Kellow et al. (2013) have published a systematic review with promising findings of the effect of dietary AGEs restriction on circulating biomarkers of vascular function in healthy subjects and diabetic patients (59). For example, in diabetic patients consuming a low-AGEs diet for six weeks, the concentration of circulating AGEs (*i.e.* CML and methylglyoxal) and vascular disease markers (*e.g.* TNF-α) were significantly decreased, whereas all parameters were increased after consuming a high-AGEs diet (26). Acutely restricting AGEs intake yielded the same results, accompanied by reduced oxidative stress and arterial stiffness, in a similar diabetic population (60). Adjusting the diet not only implies restricting the intake of AGEs-rich food but also means changing the way food is processed (7) and quit smoking (10).

The effect of dietary AGEs restriction can be enhanced when combined with moderate aerobic exercise, which prevents the internal formation of AGEs (61). In addition, some studies have investigated the effect of exercise interventions alone, including walking (62), Tai Chi (63) and endurance training (64). Semba et al. (2010) have demonstrated that higher walking speed is associated with lower CML concentrations and reduced risk of AGEs-related disease states like diabetes or hypertension (62). Secondly, a Tai Chi program of at least two hours a week for 12 months reduced systolic blood pressure relative to baseline and decreased oxidative stress when compared to the sedentary group, which can be attributed to a reduction in serum AGEs levels (63). Lastly, Maessen et al. (2017) have shown that endurance athletes have lower concentrations of the carbonyl species methylglyoxal and 3-deoxyglucosone. This was correlated with improved VO_2 peak, a prognostic marker of cardiorespiratory fitness (64). Despite conclusive evidence on the benefit of

exercise to target AGEs accumulation and its consequences in humans, the most elucidating study has been performed in a preclinical setting (65). In fact, Delbin et al. (2012) have examined the effect of exercise training on AGEs levels and vascular function in diabetic rats. The induction of diabetes led to increased CML levels and ROS production, decreased eNOS expression and NO production, and impaired arterial vasodilation. Interestingly, the exercise intervention program completely reversed these detrimental changes (65).

1.4 Aim of the study

Our research group has recently demonstrated that increased levels of circulating HMW-AGEs impair cardiac function (*i.e.* myocardial hypertrophy and fibrosis) in healthy rats, independent of RAGE activation (15). Preliminary data indicate that this adverse cardiac phenotype is related to altered functional properties of cardiomyocytes (*manuscript in preparation*). However, the exact mechanism by which HMW-AGEs mediate these adverse cellular changes and the effect of HMW-AGEs on vascular function remain unclear. Therefore, in this project, we aim to 1) examine the impact of HMW-AGEs on vascular function and 2) investigate whether previously observed cardiac dysfunction by HMW-AGEs is due to ultrastructural abnormalities in cardiomyocytes. To address these goals, rats were injected daily with either HMW-AGEs or control solution for six weeks. We hypothesize that chronic exposure to HMW-AGEs disturbs the aortic vasomotor balance by increasing superoxide formation and that HMW-AGEs alter ultrastructural cardiomyocyte organization.

2 Materials and methods

All animal experiments were performed according to the EU Directive 2010/63/EU for animal testing and were approved by the local Ethical Committee on Animal Experiments (ECAE, UHasselt, Diepenbeek, Belgium, ID 201858). Rats were group housed in standard cages with cage enrichment at the conventional animal facility of UHasselt. Rats were maintained under controlled conditions regarding temperature (22°C) and humidity (22-24%). Water and food (2018 Teklad global rodent diet, Harlan, Belgium) were provided *ad libitum* and rats were handled daily to reduce stress.

2.1 Preparation of HMW-AGEs

HMW-AGEs were prepared according to the method described by Deluyker et al. (15). Briefly, bovine serum albumin (BSA, 7 mg/ml) was incubated with glycolaldehyde dimers (90 mM; Sigma-Aldrich, Diegem, Belgium) in sterile phosphate-buffered saline (PBS, pH 7.4) for five days at 37°C. Dialysis cassettes were used to remove unreacted glycolaldehyde against PBS (3.5 kDa cut-off) (Slide-A-Lyzer® G2 Dialysis Cassette, Thermo Fisher, Erembodegem, Belgium). The solution was concentrated using Amicon® Ultra Centrifugal Filter Units (Merck, Overijse, Belgium) to obtain glycated BSA of high molecular weight (BSA-derived HMW-AGEs; 50 kDa cut-off) and filtered to remove pathogens (0.2 µm sterile filter, Sarstedt, Essen, Belgium). In parallel, BSA was dissolved in PBS (7 mg/ml) and subjected to the same dialysis-, concentration-, and filtration procedures to serve as a control solution (*i.e.* unmodified BSA). Protein concentrations of BSA-derived HMW-AGEs and unmodified BSA were verified using the Pierce™ BCA Protein Assay kit (Thermo Fisher, Erembodegem, Belgium). Both solutions were aliquoted and stored at -80°C.

2.2 Induction of the animal model

Healthy male Sprague Dawley rats (Charles River Laboratories, L'Arbresle, France) matched by age (5-6 weeks) and weight (125-150 g) were randomly assigned to daily intraperitoneal (IP) injection with 20 mg/kg/day BSA-derived AGEs (HMW-AGEs, N=12) or an equal volume of 5.5 mg/kg/day unmodified BSA (Control, N=12) for six weeks. Blood sampling was performed at the end of week 6. Just before sacrifice, invasive hemodynamic measurements were conducted to assess LV pressures. After hemodynamic measurements, rats were injected with heparin (1000 u/kg IP) and sacrificed with an overdose of Dolethal (150 mg/kg IP). Rat hearts and aortae were excised for histological examination of LV tissue and evaluation of vascular function, respectively.

2.3 Quantification of plasma AGEs levels

Blood was taken via the rat tail artery and collected in plasma tubes (Multivette® 600 Z, Sarstedt, Nümbrecht, Germany) under 3% isoflurane anesthesia. Blood samples were centrifuged at 2000 rpm for 10 min at 4°C (Micro Star 17R, VWR, Leuven, Belgium). Plasma was collected and stored at - 20°C. Plasma AGEs levels were quantified using the OxiSelect™ AGE Competitive ELISA kit (Cell Biolabs, Inc., Huissen, Netherlands), according to the manufacturer's guidelines. Briefly, plasma samples and AGE-BSA standards were added to an AGE conjugate-coated 96-well plate. Then, each well was incubated consecutively with anti-AGE antibody (1/1000) and horseradish peroxidase (HRP)-conjugated secondary antibody (1/1000). To determine unknown AGEs concentrations, absorbance was measured on a microplate reader using 450 nm as the primary wavelength and was compared with the AGE-BSA standard curve.

2.4 Hemodynamic measurements

Invasive LV hemodynamic measurements were performed in rats of both groups anesthetized with 3% isoflurane supplemented with oxygen. A pre-calibrated SPR-320 rat pressure catheter (AD instruments, Spechbach, Germany) connected to a data acquisition system (PowerLab 4/25T, AD Instruments, Spechbach, Germany) was inserted into the right carotid artery. Functional cardiac parameters including maximum pressure, mean pressure and peak time derivatives characterizing the rate of systolic contraction (Max dP/dt) and diastolic relaxation (Min dP/dt) were measured. End-diastolic pressure (EDP), the time constant of LV pressure decay during isovolumetric relaxation (Tau) and heart rate (HR) were calculated with LabChart 8 software (AD instruments, Spechbach, Germany). Catheter measurements were continued for at least 10 min to ensure stable recordings.

2.5 Evaluation of vasorelaxation using the isolated aorta technique

After sacrifice, the descending thoracic aorta was immediately isolated and placed in ice-cold Krebs solution (in mM: 118.3 NaCl, 4.7 KCl, 2.5 $CaCl_2$, 1.2 $MgSO_4$, 1.2 KH_2PO_4, 25 $NaHCO_3$, 0.026 EDTA, 5.5 glucose – pH 7.45). The aorta was cleaned of perivascular fat and connective tissue and cut into 3 mm rings, taking care not to damage the endothelium with overstretching. Aortic rings were horizontally mounted between two steel hooks, one of which was fixed and the other connected with a force transducer to record isometric tension. The hooks were placed in individual organ baths containing 40 ml Krebs solution. The bathing solution was maintained at 37°C while being continuously oxygenated throughout the experiment. Passive tension of 8 g was applied to induce optimal stretching of the aortic rings, as determined in preliminary experiments. The rings were allowed to equilibrate for 1 h. During this period, the tissue was washed every 20 min with Krebs solution. Before starting the vasorelaxation experiments, all rings were precontracted with 10^{-7} M phenylephrine (PE, Sigma-Aldrich, Diegem, Belgium) followed by the addition of 10^{-6} M acetylcholine (ACh, Sigma-Aldrich, Diegem, Belgium) to check vessel viability and endothelial integrity. Aortic rings that failed to contract in response to PE or failed to relax in response to ACh were excluded for further experiments. After testing vessel viability and integrity, the rings were washed three times with Krebs solution at 10-min intervals and were ready for studying relaxation responsiveness. Briefly, aortic rings with intact endothelium were precontracted by adding PE (10^{-7} M) to the organ bath, and the contraction was allowed to reach a stable plateau phase. The relaxation responses to cumulative doses of ACh (final bath concentrations: 10^{-10}-10^{-5} M) or sodium nitroprusside (SNP, final bath concentrations: 10^{-10} to 10^{-6} M, Sigma-Aldrich, Diegem, Belgium) were tested to assess endothelium-dependent and endothelium-independent relaxation of aortic rings, respectively. In addition, ACh-induced relaxation was evaluated in the presence of either 10^{-4} M N(ω)-nitro-L-arginine methyl ester (L-NAME, Sigma-Aldrich, Diegem, Belgium), to assess eNOS activity, or 10^{-5} M indomethacin (INDO, Sigma-Aldrich, Diegem, Belgium) dissolved in dimethyl sulfoxide (DMSO), to investigate the role of cyclooxygenase (COX) in ACh-induced relaxation. Both inhibitors were added 30 min before precontraction with PE (10^{-7} M), followed by investigating the vasorelaxation response to cumulative doses of ACh (final bath concentrations: 10^{-10} to 10^{-5} M). To determine the contribution of superoxide radicals, a similar dose-response curve to ACh after PE-induced precontraction was performed in the presence of superoxide dismutase (SOD, 150 kU, Sigma-Aldrich, Diegem, Belgium), which was added 30 min before the addition of PE (10^{-7} M). All sets of experiments were conducted in series so that each aortic ring was subjected to all conditions, separated by a 30-min washout.

Tensions were measured by an isometric force transducer (MLT 050/A, AD Instruments, Spechbach, Germany) connected to a data acquisition system (PowerLab 4/25T, AD Instruments, Germany). Dose-response curves were recorded for 4 min after each addition of ACh or SNP and were analyzed with LabChart software (v 8.1.13, AD instruments, Spechbach, Germany). Vasorelaxation responses to ACh and SNP were expressed as the percentage of relaxation relative to PE-induced contraction.

2.6 Assessment of cardiomyocyte organization by histology and electron microscopy

LV tissue was processed for both light microscopic (LM) and electron microscopic (EM) examination of cardiomyocyte organization. The tissues of control and HMW-AGEs animals were fixed overnight with 2% glutaraldehyde in 0.05 M cacodylate buffer at 4°C, post-fixed in 2% osmium tetroxide and stained with 2% uranyl acetate in 10% acetone. Samples were dehydrated in a graded series of acetone and embedded in Araldite according to the pop-off method. Semi-thin sections were stained with toluidine blue and adequately prepared LV tissue was randomly selected for LM examination. Subsequently, ultra-thin sections were cut and mounted on formvar-coated grids, counterstained with uranyl acetate and lead citrate, and were imaged in a Philips EM 208 transmission electron microscope (Philips, Eindhoven, Netherlands). Random EM pictures of cardiomyocytes with a visible nucleus were taken at 1800x magnification. In LM pictures, mitochondrial area (dark blue color) was measured using the threshold tool in ImageJ and expressed as a percentage of total cell area (66). In EM pictures, morphometric analysis of intracellular cardiomyocyte organization was performed. Mitochondrial density was calculated as the ratio of the number of mitochondria to the total cell area. Mitochondrial, myofilament, nuclear and cytoplasmic fractions were measured by grid-point analysis in ImageJ, counting every point (distance = 2 µm) at the intersection of horizontal and vertical lines (66). Data are presented as the percentage of total grid points. All samples were coded and the observer was blinded for group allocation during image analysis.

2.7 Statistical analysis

Statistical analysis was performed using GraphPad Prism (GraphPad software, version 5.01, San Diego, CA, USA). All data are expressed as the mean ± standard error of the mean (SEM). Normal distribution of data was verified by the D'Agostino-Pearson normality test. All data sets passed normality and were compared with the unpaired t-test. To analyze aortic vasorelaxation in the HMW-AGEs group and control group, dose-response curves were fitted by nonlinear regression and compared using two-way ANOVA with correction for multiple comparisons. From these curves, the maximal response (E_{max}) to ACh or SNP and dose required to obtain half-maximal response (EC_{50}) were calculated. The unpaired t-test was applied to compare the E_{max} and EC_{50} values of both groups. The sample size is represented as 'n', indicating the number of aortic rings or cardiomyocytes, or 'N', indicating the number of animals. A value of $P<0.05$ was considered significant.

3 Results

3.1 HMW-AGEs injections increase circulating AGEs levels and intracardiac pressure

Blood samples were taken six weeks after the first injection with BSA-derived HMW-AGEs (HMW-AGEs group) or unmodified BSA (control group). Plasma AGEs content was measured to validate the animal model. The HMW-AGEs group showed a significant increase in total circulating AGEs levels when compared to the control group (111 ± 3 µg/ml vs. 84 ± 5 µg/ml respectively, P<0.001; Figure 3).

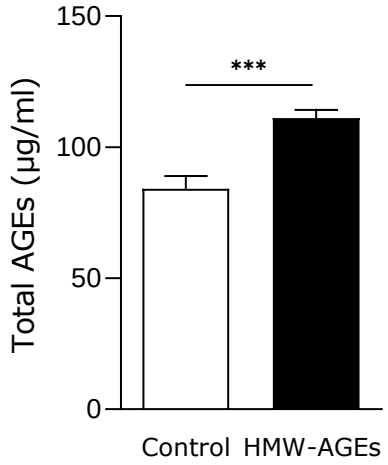

Figure 3: Total circulating AGEs levels. AGEs concentration (µg/ml) was measured in plasma samples from control (N=10) and HMW-AGEs (N=12) animals by ELISA after six weeks of daily injections. Data are presented as mean ± SEM. ***P<0.001. *AGEs = advanced glycation end products.*

To examine cardiac function, *in vivo* LV hemodynamic measurements were performed just before sacrifice. As shown in Table 1, maximum and mean LV pressures were significantly increased in HMW-AGEs animals compared to control animals (P<0.05). Other parameters including HR, EDP, Max dP/dt, Min dP/dt and time constant Tau were similar among both groups.

Table 1: LV hemodynamic parameters after six weeks of injections.

Hemodynamic parameters	**Week 6**	
	Control	HMW-AGEs
HR (bpm)	335 ± 7	355 ± 10
Max pressure (mmHg)	91 ± 3	100 ± 4*
Mean pressure (mmHg)	36 ± 2	41 ± 2*
EDP (mmHg)	4.8 ± 1.6	6.3 ± 1.2
Max dP/dt (mmHg/s)	6063 ±268	6187 ± 377
Min dP/dt (mmHg/s)	-6961 ± 538	-6737 ± 459
Tau (s)	0.011 ± 0.001	0.014 ± 0.003

LV measurements were performed using a pressure catheter inserted in the right carotid artery of control (N=10) and HMW-AGEs (N=10) animals. Data are presented as mean ± SEM. *P<0.05. *LV = left ventricular, HR = heart rate, EDP = end-diastolic pressure, Max dP/dt = maximum rate of pressure rise, Min dP/dt = minimum rate of pressure decline, Tau = time constant of LV pressure decay during isovolumetric relaxation.*

3.2 HMW-AGEs enhance contraction and impair endothelium-dependent relaxation

After precontraction with PE, relaxation responses to cumulative doses of ACh and SNP were assessed in aortic rings of both groups to investigate endothelium-dependent and endothelium-independent relaxation, respectively. The contractile response to a single dose of PE, represented by tension development, was significantly higher in the HMW-AGEs group compared to the control group (2.059 ± 0.083 g vs. 1.354 ± 0.075 g respectively, P<0.0001), as shown in Figure 4.

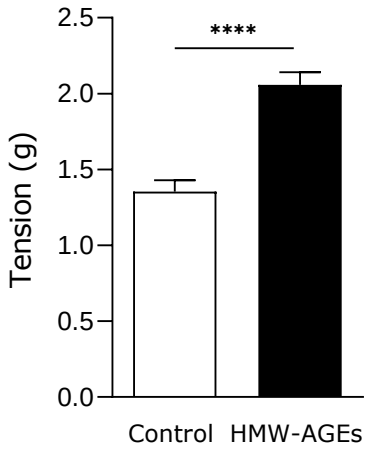

Figure 4: Contractile response to a single dose of PE. Rat aortic rings of control (n_{rings}=54) and HMW-AGEs (n_{rings}=60) animals were precontracted with 10^{-7} M PE. The contractile response is expressed as the magnitude of tension development in grams. Aortic rings were obtained from 9 control and 11 HMW-AGEs animals. Data are presented as mean ± SEM. ****P<0.0001. *PE = phenylephrine.*

ACh and SNP caused dose-dependent relaxation in aortic rings of both groups (Figure 5). In HMW-AGEs rings, ACh-induced relaxation was impaired, demonstrating a significant rightward shift of the dose-response curve at low doses compared to control rings (10^{-9} M P<0.01, 10^{-8} M P<0.0001 and 10^{-7} M P<0.05; Figure 5A).

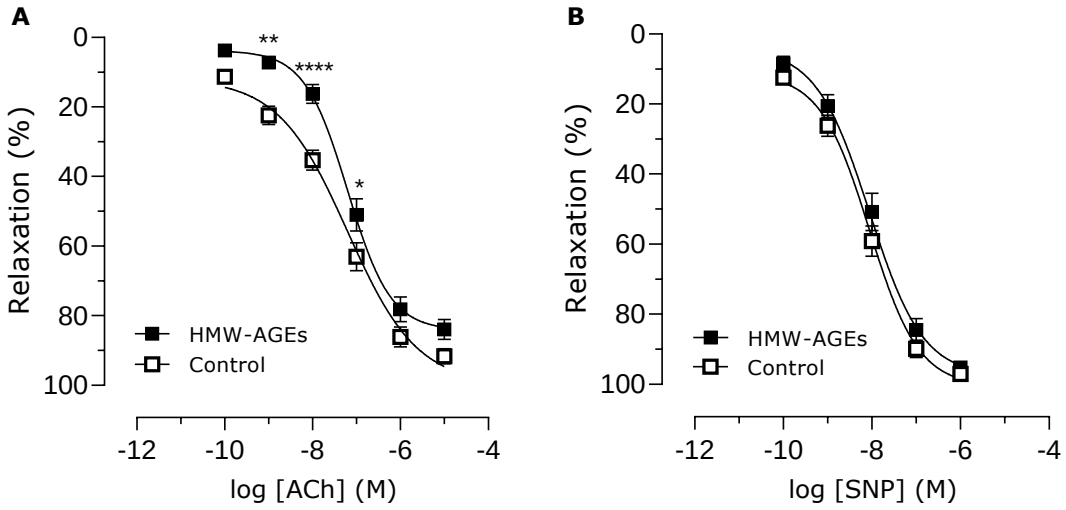

Figure 5: Endothelium-dependent and endothelium-independent relaxation. A. Relaxation response to cumulative doses of ACh (final bath concentrations: 10^{-10}-10^{-5} M) in rat aortic rings from 10 control (n_{rings}=26) and 9 HMW-AGEs (n_{rings}=32) animals. **B.** Relaxation response to cumulative doses of SNP (final bath concentrations: 10^{-10}-10^{-6} M) in rat aortic rings of 11 control (n_{rings}=28) and 8 HMW-AGEs (n_{rings}=28) animals. The response is expressed as a percentage of PE-induced precontraction (10^{-7} M). Data points are presented as mean ± SEM. *P<0.05, **P<0.01, ****P<0.0001. *ACh = acetylcholine, SNP = sodium nitroprusside. PE = phenylephrine.*

As summarized in Table 2, the HMW-AGEs group demonstrated a significant decline of E_{max} to ACh compared with control (83.94 ± 2.80% vs. 91.65 ± 2.08% respectively, P<0.05). Moreover, the EC_{50} value tended to be higher in HMW-AGEs animals (-7.071 ± 0.089 M vs. -7.330 ± 0.139 M in control group, P=0.0529). In contrast, no change of aorta responsiveness to SNP was observed (Figure 5B). In addition, there was no statistical difference in E_{max} and EC_{50} values for SNP between both groups (Table 2).

Table 2: E_{max} and EC_{50} values of ACh- and SNP-induced relaxation.

Groups	E_{max} (%)	$LogEC_{50}$ (M)
ACh		
Control	91.65 ± 2.08	-7.330 ± 0.139
HMW-AGEs	83.94 ± 2.80 *	-7.071 ± 0.089
Control + SOD	94.29 ± 1.19	-7.532 ± 0.147
HMW-AGEs + SOD	92.31 ± 2.95 #	-7.415 ± 0.116 #
SNP		
Control	97.00 ± 0.95	-8.072 ± 0.112
HMW-AGEs	95.15 ± 1.04	-7.970 ± 0.107

Values of maximal relaxation (E_{max}) and the dose required to obtain half-maximal response (EC_{50}) were derived from dose-response curves generated by nonlinear regression analysis. E_{max} was calculated as a percentage of PE-induced contraction. EC_{50} is expressed as the logarithm ($LogEC_{50}$) of molar concentration (M). Sample size ACh condition: n_{rings} control=26, n_{rings} HMW-AGEs=32, n_{rings} control+SOD=13, n_{rings} HMW-AGEs+SOD=22; sample size SNP condition: n_{rings} control=28, n_{rings} HMW-AGEs=28. Data are presented as mean ± SEM. *P<0.05 vs. control, #P<0.05 vs. HMW-AGEs. *ACh = acetylcholine, SNP = sodium nitroprusside, PE = phenylephrine, SOD = superoxide dismutase.*

3.3 SOD pretreatment reverses HMW-AGEs-induced impairment of relaxation

To examine the underlying mechanism of HMW-AGEs-induced impairment of relaxation, aortic rings of HMW-AGEs and control animals were preincubated with the eNOS inhibitor L-NAME, the enzymatic antioxidant SOD or the COX inhibitor INDO. Subsequently, dose-response curves to ACh were obtained. As expected, L-NAME substantially blocked relaxation in both groups (control: 10^{-9} M, $P<0.05$; 10^{-8}-10^{-5} M, $P<0.0001$ and HMW-AGEs: 10^{-7}-10^{-5} M, $P<0.0001$). However, there was no statistical difference between the aortic rings of HMW-AGEs and control animals (Figure 6A and B).

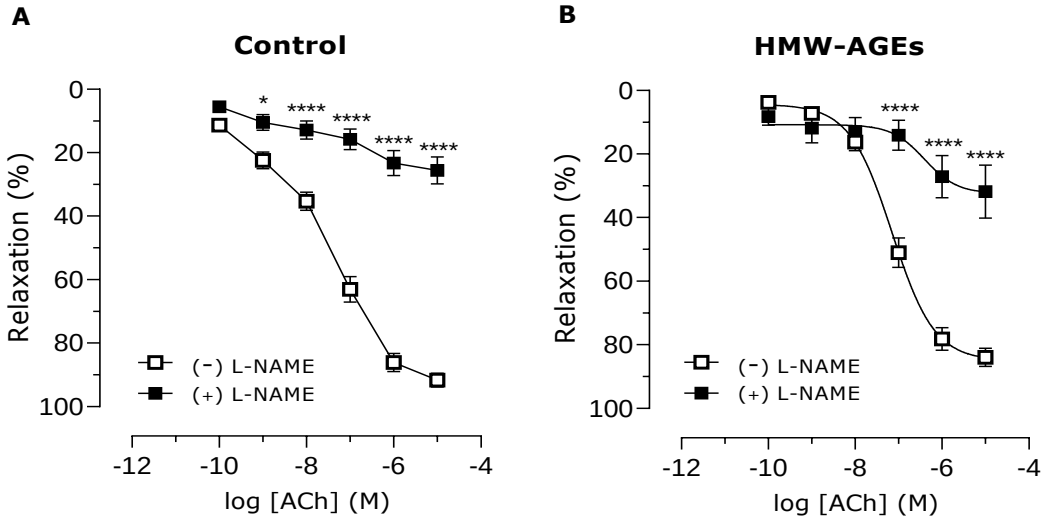

Figure 6: Effect of L-NAME on ACh-induced relaxation. Rat aortic rings from control **(A)** and HMW-AGEs **(B)** animals were preincubated with 10^{-4} M L-NAME for 30 min (n_{rings} control=15 and n_{rings} HMW-AGEs=5) or left untreated (n_{rings} control=26 and n_{rings} HMW-AGEs=32). The relaxation response to cumulative doses of ACh is expressed as a percentage of PE-induced contraction. Aortic rings preincubated with L-NAME were obtained from 9 control and 4 HMW-AGEs animals**.** Data points are presented as mean ± SEM. *P<0.05, ****P<0.0001. *ACh = acetylcholine, PE = phenylephrine, L-NAME = N(ω)-nitro-L-arginine methyl ester.*

While preincubation with SOD had no effect on ACh-induced relaxation of aortic rings from control animals (Figure 7A), it restored relaxation in aortic rings from HMW-AGEs animals. More specifically, a leftward shift of the dose-response curve can be observed at 10^{-8} M ($P<0.05$) and 10^{-7} M ACh ($P<0.001$) (Figure 7B). In line with this finding, SOD pretreatment significantly reduced the EC_{50} value of aortic rings from the HMW-AGEs group, as shown in Table 2 (-7.415 ± 0.116 M vs. -7.071 ± 0.089 M in the presence and absence of SOD respectively, $P<0.05$). In addition, E_{max} was significantly increased in the presence of SOD (92.31 ± 2.95% with SOD vs. 83.94 ± 2.80% without SOD, $P<0.05$).

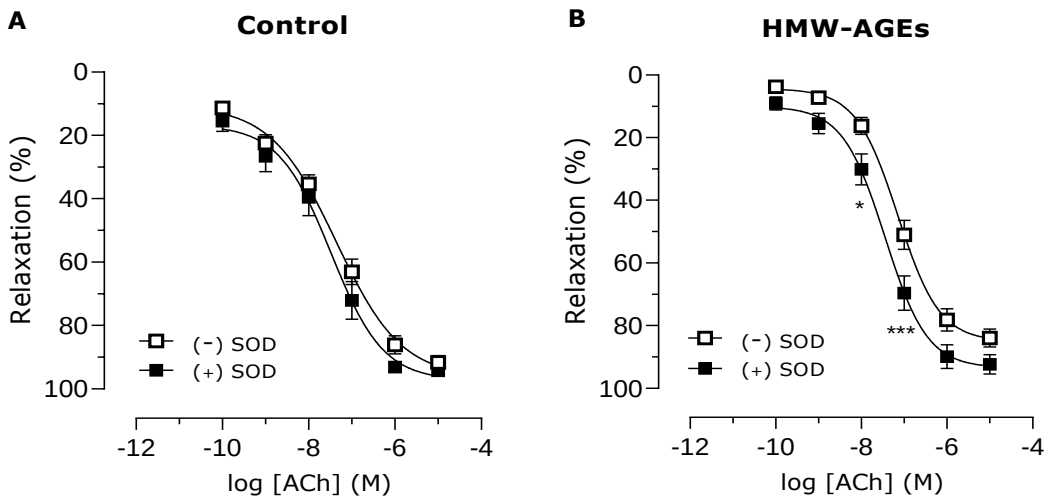

Figure 7: Effect of SOD on ACh-induced relaxation. Rat aortic rings from control **(A)** and HMW-AGEs **(B)** animals were preincubated with 150 kU SOD for 30 min (n_{rings} control=13 and n_{rings} HMW-AGEs=22) or left untreated (n_{rings} control=26 and n_{rings} HMW-AGEs=32). The relaxation response to cumulative doses of ACh is expressed as a percentage of PE-induced contraction. Aortic rings preincubated with SOD were obtained from 5 control and 6 HMW-AGEs animals**.** Data points are presented as mean ± SEM. *P<0.05, ***P<0.001. *PE = phenylephrine, ACh = acetylcholine. SOD = superoxide dismutase.*

After preincubation with INDO, significant inhibition of relaxation in response to high doses of ACh was observed in aortic rings from the control group (10^{-7}-10^{-5} M, P<0.0001), as shown in Figure 8A. In contrast, there was no difference in the HMW-AGEs group at these doses (Figure 8B). In response to low doses of ACh, INDO-pretreated aortic rings of HMW-AGEs animals showed a significant increase in relaxation (10^{-10} M, P<0.05; 10^{-9} and 10^{-8} M, P<0.0001).

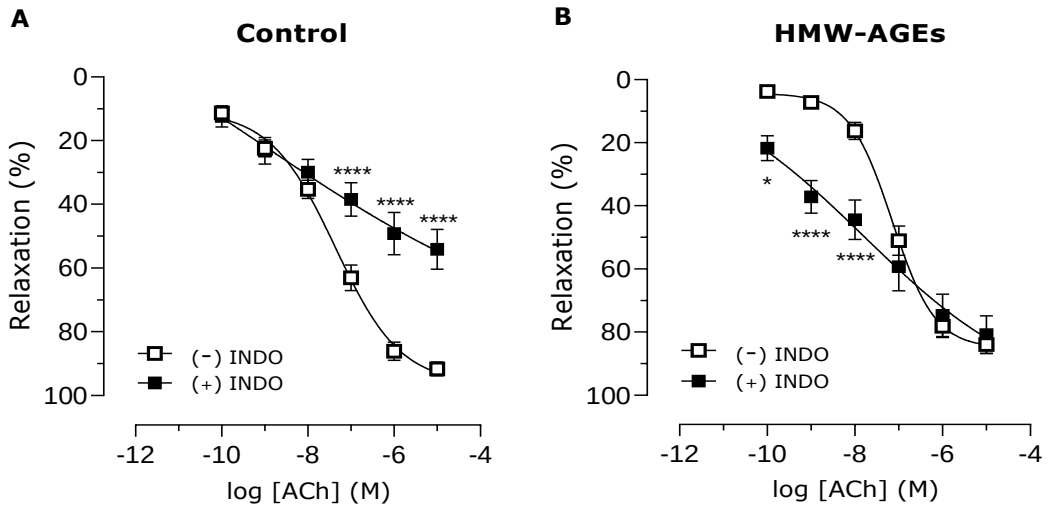

Figure 8: Effect of INDO on ACh-induced relaxation. Rat aortic rings from control **(A)** and HMW-AGEs **(B)** animals were preincubated with 10^{-5} M INDO for 30 min (n_{rings} control=12 and n_{rings} HMW-AGEs=13) or left untreated (n_{rings} control=26 and n_{rings} HMW-AGEs=32). The relaxation response to cumulative doses of ACh is expressed as a percentage of PE-induced contraction. Aortic rings preincubated with INDO were obtained from 5 control and 8 HMW-AGEs animals**.** Data points are presented as mean ± SEM. *P<0.05, ****P<0.0001. *ACh = acetylcholine, PE = phenylephrine, INDO = indomethacin.*

3.4 HMW-AGEs increase cytoplasmic fraction and reduce mitochondrial number

Morphometric analyses with LM and EM were performed on LV tissue from HMW-AGEs and control animals to evaluate the ultrastructural organization of cardiomyocytes. LM examination of toluidine blue-stained sections revealed that mitochondrial area was significantly reduced in cardiomyocytes from HMW-AGEs animals compared to control animals (21 ± 0.3% vs. 24 ± 0.5% respectively, P<0.0001; Figure 9A and B).

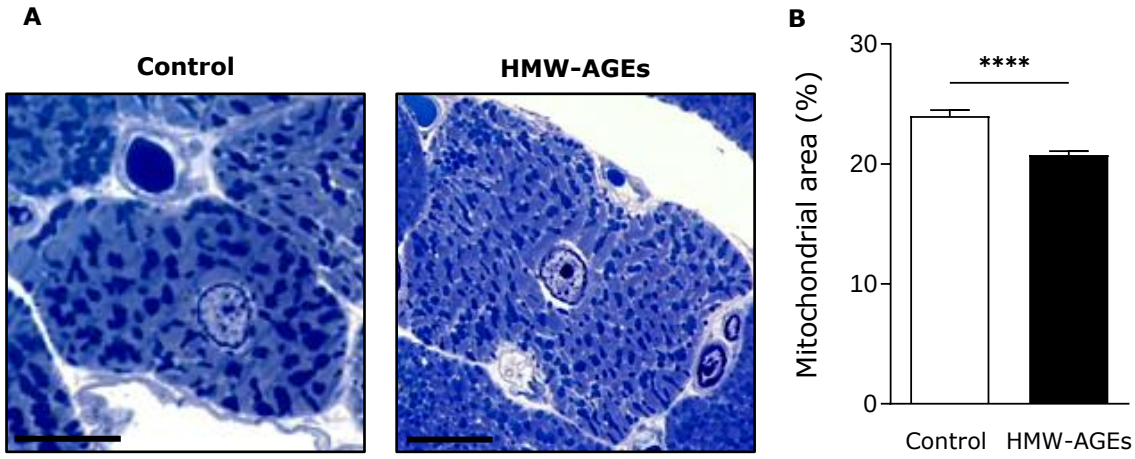

Figure 9: LM examination of mitochondrial area. A. Toluidine blue staining of LV cardiomyocytes from control (left panel) and HMW-AGEs (right panel) animals showing mitochondria (dark blue) and myofilaments/cytoplasm (light blue). **B.** Quantification of mitochondrial area in control (n_{cells}=90) and HMW-AGEs (n_{cells}=165) cardiomyocytes was performed via thresholding in ImageJ. Mitochondrial area is expressed as a percentage of total cell area. Cells were obtained from 6 control and 6 HMW-AGEs animals. Data are presented as mean ± SEM. ****P<0.0001. Scale bars: 20 µm.

EM analysis of LV cardiomyocytes confirmed these findings, with Figure 10B demonstrating a significant decrease of mitochondrial fraction in the HMW-AGEs group compared to control (33 ± 0.9% vs. 36 ± 1.2% respectively, P<0.05). Representative EM pictures of cardiomyocytes from control and HMW-AGEs animals are illustrated in Figure 10A. Cardiomyocytes from control animals showed numerous mitochondria interspersed between regularly organized myofilaments. The integrity of this network was altered in cardiomyocytes from HMW-AGEs animals, presenting greater space between myofilaments. Moreover, a perinuclear halo could be observed, which was rarely seen in the control group. This appearance was associated with a significant increase of cytoplasmic fraction in cardiomyocytes of HMW-AGEs animals, defined as the area without mitochondria or myofilaments (15 ± 1.3% vs. 11 ± 0.6% in control, P<0.01; Figure 10C). Quantification of myofilament fraction revealed that there was no statistically significant difference between HMW-AGEs and control cardiomyocytes (Figure 10D). In addition, the nuclear fraction was similar in both groups (Figure 10E). Mitochondrial density, calculated as the ratio of the number of mitochondria to the total cell area, was measured to examine whether the reduction of the mitochondrial area was due to a reduction in mitochondrial number. Figure 10F shows that mitochondrial density was significantly decreased in cardiomyocytes from HMW-AGEs animals compared to control (0.40 ± 0.1 a.u. vs. 0.46 ± 0.1 a.u. respectively, P<0.05).

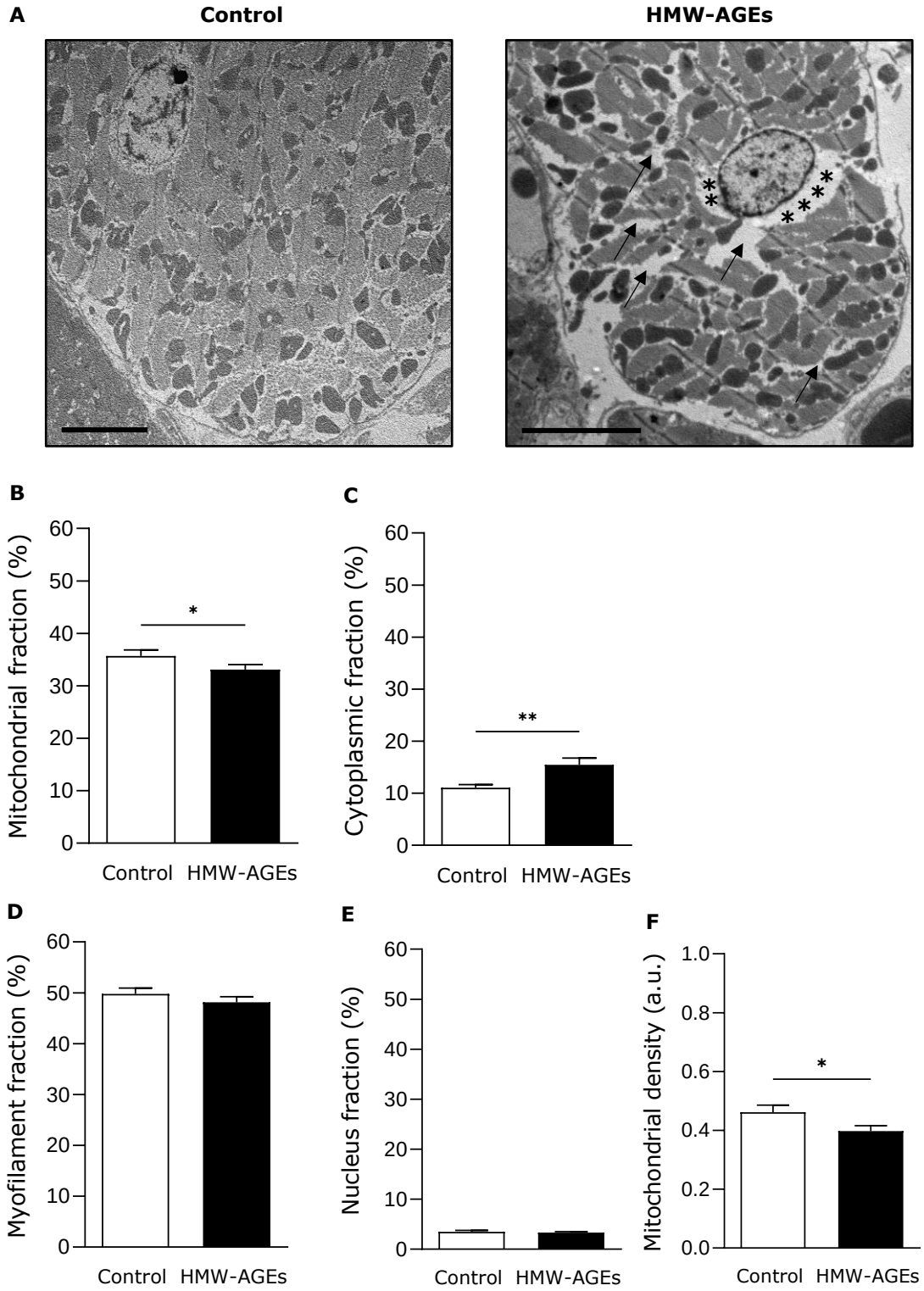

Figure 10: Morphometric analysis of cardiomyocyte organization by EM. A. Representative electron micrographs of LV cardiomyocytes from control and HMW-AGEs animals. Cardiomyocytes of control animals (left panel) showed typical intracellular organization of myofilaments (light grey), mitochondria (dark grey) and cytoplasm (white). Cardiomyocytes from HMW-AGEs animals (right panel) displayed greater cytoplasmic space between mitochondria and myofilaments (arrows), and a perinuclear halo (*). **B-E.** Quantification of mitochondrial **(B)**, cytoplasmic **(C)**, myofilament **(D)** and nuclear **(E)** fractions in cardiomyocytes from control (n_{cells}=23) and HMW-AGEs (n_{cells}=30) animals using grid-point analysis in ImageJ. Intracellular fractions are expressed as a percentage of total grid points. **F.** Mitochondrial density calculated as the ratio of mitochondrial number to total cell area. Cells were obtained from 6 control and 6 HMW-AGEs animals. Data are presented as mean ± SEM. *P<0.05, **P<0.01. Magnification: 1800×. Scale bars: 5 µm.

4 Discussion

Distinguishing AGEs compounds according to molecular weight is essential to understand their distinct role in cardiovascular dysfunction. In this study, we show that HMW-AGEs significantly increase intracardiac pressure and impair NO-mediated endothelium-dependent relaxation in rat aortic rings through superoxide formation. Furthermore, we indicate that ultrastructural changes and reduced mitochondrial number in cardiomyocytes underlie HMW-AGEs-induced cellular remodeling.

4.1 Increased circulating HMW-AGEs levels lead to intracardiac pressure overload

This project is based on an animal model that mimics chronic HMW-AGEs exposure *in vivo*, as described in our recently published study (15). For a period of six weeks, we daily injected HMW-AGEs to healthy male Sprague-Dawley rats and compared this group with control rats receiving unmodified BSA. As expected, circulating AGEs levels were significantly increased in HMW-AGEs animals, which validates the animal model and ensures the reliability of all experiments performed in this study. We have demonstrated a similar increase in AGEs levels before (15), indicating that the induction of this animal model is part of routine practice in our lab. Exogenous administration of AGEs has been performed in many other studies, although these did not focus on HMW-AGEs. Vlassara et al. (1992) were the first to report that AGEs injections to healthy rats can be used as a model for studying the pathogenicity of AGEs (26). Other models for AGEs research include those administering AGEs via the drinking water (67) or via AGEs-enriched diets (68). However, oral AGEs administration is associated with lower absorption and thus decreased plasma AGEs levels when compared to AGEs injection (67).

Our research group has recently evaluated the impact of HMW-AGEs on cardiac structure and function by conventional echocardiography. Elevated circulating HMW-AGEs levels result in increased LV wall thickness and diameters, which are typical signs of wall hypertrophy and diastolic dysfunction (15). In this study, we performed LV hemodynamic measurements to complement these echocardiographic data. HMW-AGEs animals showed significantly increased maximum and mean LV pressures. This pressure overload forces the heart to eject blood against a high LV afterload so that the cardiac muscle becomes hypertrophic, which is in accordance with the previously observed increase in wall thickness (15). In addition, Candido et al. (2003) have reported that diabetic rats with increased AGEs content demonstrate higher systolic blood pressure compared to healthy controls (69), which confirms the link between increased HMW-AGEs levels and pressure overload as observed in this study.

4.2 HMW-AGEs disturb the vasomotor balance in isolated rat aortae

The main function of the vascular endothelium is regulating the vasomotor tone through the balanced secretion of relaxing and contracting factors that influence vascular smooth muscle cells (70). In physiological conditions, the process of endothelium-dependent vascular relaxation is mainly mediated by NO. The classic pathway of NO release starts with the interaction between ACh and its G-protein coupled muscarinic M3 receptor on endothelial cells. This interaction leads to the activation of phospholipase C, which facilitates the conversion of phosphatidylinositol 4,5-bisphosphate (PIP_2) into inositol trisphosphate (IP_3) and diacylglycerol (DAG), and promotes calcium influx in endothelial cells. The resultant increase of intracellular calcium stimulates eNOS to synthesize NO from the amino acid L-arginine (71)**.** NO compounds diffuse into vascular smooth muscle cells, where they stimulate cyclic guanosine monophosphate (cGMP) production by guanylate cyclase. The subsequent reduction of intracellular calcium forces vascular smooth muscles to relax (72). Although the impact of LMW-AGEs on vasorelaxation has been well documented (73), the role of HMW-AGEs remains unclear.

In this study, we show that HMW-AGEs significantly reduce E_{max} and adversely shift the typical dose-response curve of ACh. In addition, the EC_{50} value, a measure for agonist potency, tend to be increased in aortic rings from HMW-AGEs animals compared to control animals. This indicates that the aortic sensitivity for ACh is likely to be attenuated by HMW-AGEs, although statistical significance was not reached. To confirm the involvement of the endothelium, relaxation in response to SNP was examined. SNP is a NO donor which mediates relaxation of vascular smooth muscle cells without the contribution of endothelial cells. Our results demonstrate that SNP-induced relaxation is similar for both groups, indicating that HMW-AGEs affect endothelial function but do not cause a generalized reduction of vascular smooth muscle responsiveness. The observed data are in line with animal studies examining the effect of LMW-AGEs on the relaxation capacity of isolated rat aortic rings. Chen et al. (2008) have demonstrated that chronic injections with LMW-AGEs inhibit endothelium-dependent but not endothelium-independent, as shown by reduced E_{max} and increased EC_{50} values in response to ACh and not SNP (74). Similarly, acute exposure of aortic rings to LMW-AGEs for 24 h decreased ACh-induced vasorelaxation in a dose-dependent manner, whereas the response to SNP remained unchanged (75). LMW-AGEs not only impair vasorelaxation but also strengthen vascular contraction in response to PE, as reported by Eid et al. (2018) (76). Furthermore, they increase the expression of the potent vasoconstrictor ET-1 in aortic endothelial cells (39). Consistent with this observation, we describe a 35% increase of maximal tension development in aortic rings from HMW-AGEs animals compared to control animals. However, we must emphasize that contraction was measured in response to a single dose of PE (*i.e.* 10^{-7} M). Hence, assessing relaxation in response to cumulative doses of PE is necessary to strengthen this finding and draw conclusions on how HMW-AGEs exaggerate vascular contraction; through changes in α1 adrenergic signaling or not.

4.3 Superoxide formation is the underlying mechanism of impaired relaxation

Since NO is essential for the functionality of the endothelium, it is reasonable to think that HMW-AGEs disturb the vasomotor balance by reducing NO bioavailability (34)**.** Different mechanisms of how AGEs reduce NO bioavailability have been suggested, such as lower NO production due to decreased eNOS activity or NO inactivation secondary to the formation of superoxide radicals (24). To investigate the mechanism by which HMW-AGEs mediate endothelial dysfunction, relaxation responses were measured in the presence of the eNOS inhibitor L-NAME and antioxidant enzyme SOD. Interestingly, SOD pretreatment fully restored endothelium-dependent relaxation in aortic rings from HMW-AGEs animals, while this was not observed for control animals. In addition, we show that the degree of inhibition of relaxation by L-NAME was not different between both groups. These data confirm our hypothesis that HMW-AGEs does impair aortic vasorelaxation by increasing superoxide formation, rather than by reducing eNOS activity. This suggests that HMW-AGEs inactivate or degrade adequately-produced NO compounds.

Our finding is of particular interest since experiments performed in diabetic rats have demonstrated that the aortic endothelium is extremely vulnerable for oxidative damage (77). Moreover, it has been described that AGEs double the production of oxygen-derived free radicals in rat aortic tissue (67) as well as in human endothelial cells (78). Superoxide radicals react with vascular NO, leading to the formation of peroxynitrite and quenching of bioactive NO molecules (37, 79). Indeed, Su et al. (2013) have demonstrated that acute exposure to AGEs decreases the aortic NO content due to increased superoxide formation (75). As already mentioned, AGEs can promote ROS production through their interaction with endothelial RAGE. It is assumed that subsequent activation of signaling cascades inside the endothelium leads to superoxide formation by NADPH oxidases and eventually impaired vasodilation (35, 80). However, our research group has recently demonstrated that RAGE does not necessarily mediate the deleterious effects of HMW-AGEs. Whether HMW-AGEs impair vascular function through endothelial RAGE activation remains to be determined in future experiments.

Besides NO, PGI_2 is another relaxing factor secreted by endothelial cells. PGI_2 compounds are arachidonic acid metabolites formed by COX enzymes (81). It can be hypothesized that the inhibition of endothelium-dependent relaxation by HMW-AGEs involves decreased PGI_2 production. Therefore, ACh-induced vasorelaxation was assessed in the presence of the COX inhibitor INDO. In this study, we show that INDO significantly reduces relaxation in aortic rings from control animals. However, this effect was smaller than the reduction induced by L-NAME, which confirms that NO is more important than PGI_2 for endothelium-dependent aortic relaxation in physiological circumstances. Remarkably, the inhibitory effect of INDO on vasorelaxation was less pronounced in aortic rings from HMW-AGEs animals at higher doses of ACh and was even increased at lower doses. This observation can be explained by the fact that superoxide radicals stimulate COX enzymes to produce PGI_2 (82, 83). This is consistent with our data indicating a key role for superoxide radicals in the impairment of vasorelaxation induced by HMW-AGEs. Thus, in our study, the inhibitory effect of INDO is blunted by increased PGI_2 production secondary to superoxide formation in aortic rings of HMW-AGEs animals.

4.4 HMW-AGEs cause adverse ultrastructural remodeling in cardiomyocytes

The cardiac muscle has a unique ultrastructure consisting of myofilaments (*e.g.* actin and myosin) to mediate contraction and cytoskeletal proteins (*e.g.* desmin) to maintain myofilament organization (84). Their interaction is essential for proper cardiac function because cytoskeletal changes can lead to contractile dysfunction of cardiomyocytes (85). Cardiomyocyte contraction depends on the efficiency of excitation-contraction coupling. During this process, calcium enters cardiac cells through L-type calcium channels located on the cell membrane in response to an action potential. This calcium influx triggers massive calcium release from the ryanodine receptor, located on the membrane of the sarcoplasmic reticulum, called calcium-induced calcium release. This increase of intracellular calcium is essential to elicit contraction of the cardiomyocyte (86).

Our research group has recently demonstrated that HMW-AGEs cause reduced and slower unloaded cell shortening and decrease L-type calcium current density, resulting in altered excitation-contraction coupling (*manuscript in preparation*). However, the exact cause of cardiomyocyte dysfunction induced by HMW-AGEs currently remains unexplained. In this study, we show that HMW-AGEs significantly increase the cytoplasmic space, thereby disrupting the typical cardiomyocyte ultrastructure. On the other hand, the myofilament fraction was similar in both groups, which suggests that cardiomyocyte dysfunction induced by HMW-AGEs is more likely to be associated with cytoskeletal changes rather than alterations in myofilament abundance. In this context, Diguet et al. (2011) have demonstrated that LMW-AGEs disrupt the cytoskeletal network in cardiomyocytes of mice with dilated cardiomyopathy by modifying desmin filaments (87). Furthermore, desmin-null mice show loss of sarcomeric integrity and develop cardiac hypertrophy (88), as also seen in HMW-AGEs-injected animals (15). Based on these results, it is tempting to speculate that HMW-AGEs disrupt desmin organization, but this requires further investigation. In addition, cytoskeletal changes have been shown to modulate L-type calcium channel activity, which explains the decrease of calcium influx induced by HMW-AGEs, observed in previous experiments performed by our research group.

Mitochondria are crucial for proper cardiomyocyte contraction through their production of adenosine triphosphate (ATP) via oxidative phosphorylation (86). Interestingly, we show that mitochondrial area is significantly decreased in cardiomyocytes from HMW-AGEs animals. This decrease is due to a reduction in mitochondrial number rather than being a consequence of increased cytoplasmic area, which indicates that HMW-AGEs stimulate mitophagy in cardiomyocytes. Mitophagy describes the selective elimination of damaged mitochondria to maintain cellular homeostasis (89). The association between AGEs and mitophagy has been reported before. Zha et al. (2018) have recently demonstrated that *in vitro* LMW-AGEs treatment of neonatal rat cardiomyocytes increases the expression of proteins involved in mitophagy through enhanced ROS production (90). In addition, AGEs-induced RAGE signaling via the PI3K/AKT/mTOR pathway seems to be implicated in the process of AGEs-induced mitophagy in cultured cardiomyocytes (91, 92). Taken together, our results suggest that HMW-AGEs damage mitochondria, resulting in their degradation through mitophagy. It can be hypothesized that the subsequent reduction in mitochondrial number leads to functional changes (*e.g.* lower ATP production), thereby impairing cardiomyocyte contraction. However, this hypothesis should be tested in future research.

4.5 Limitations

There are several limitations that should be noted. Echocardiography was not performed in this study due to practical constraints. Echocardiographic measurements would complement our hemodynamic data to fully characterize cardiac function. However, our research group has already shown that elevated circulating HMW-AGEs levels are associated with echocardiographic abnormalities, being increased LV wall thickness and LV chamber volumes (15).

Second, the passive tension of 8 g to induce optimal baseline stretching of aortic rings was determined in preliminary experiments on aortic rings from control rats, but not on aortic rings from HMW-AGEs rats. However, each tissue has a length at which it responds best (93). Therefore, the optimal passive tension could be different for aortic tissue from HMW-AGEs-injected rats compared to control rats. In this study, vasorelaxation responses were expressed as the percentage of relaxation relative to PE-induced contraction, which means that we have largely addressed this limitation.

In addition, we did not examine the area or number of mitochondrial subpopulations (*i.e.* perinuclear, intermyofibrillar and subsarcolemmal mitochondria). Analyzing these subpopulations in the future would give a better understanding of the effect of HMW-AGEs on cardiomyocytes since mitochondrial subpopulations differ in function (94).

A final limitation could be the clinical relevance of the HMW-AGEs solution, which was prepared by incubating BSA with glycolaldehyde dimers at a concentration of 90 mM. This is about 90 times higher than the concentration measured in humans (95). Finally, HMW-AGEs injections and the related experiments are performed in rats, making the translation to the clinical situation rather difficult due to interspecies differences.

5 Conclusion

Over the last decades, growing evidence has been supporting the contribution of AGEs to cardiovascular disease. Our research group has recently demonstrated that increased levels of circulating HMW-AGEs impair cardiac function in healthy rats. Preliminary data indicate that HMW-AGEs also alter cardiomyocyte structure and function. Therefore, the aim of this study was to elucidate the exact mechanism by which HMW-AGEs mediate adverse cardiomyocyte changes and to examine the impact of HMW-AGEs on vascular function.

The present study has revealed some interesting findings. We show that increased circulating HMW-AGEs levels lead to intracardiac pressure overload. Moreover, this adverse cardiac phenotype is related to a disturbance of the vasomotor balance in isolated rat aortae, illustrated by enhanced contraction and impaired endothelium-dependent relaxation in HMW-AGEs animals. Interestingly, SOD pretreatment completely reversed the impairment of endothelium-dependent relaxation induced by HMW-AGEs, which indicates that this impairment can be attributed to superoxide formation. Finally, we show that HMW-AGEs cause adverse ultrastructural remodeling in cardiomyocytes, as demonstrated by an increase in cytoplasmic fraction and a reduction of the mitochondrial number in cardiomyocytes from HMW-AGEs animals. These data strongly suggest that ultrastructural remodeling is involved in HMW-AGEs-induced cardiomyocyte dysfunction. Taken together, our study is the first to show that HMW-AGEs induce cardiovascular dysfunction in a chronic non-pathological setting.

This project creates opportunities for future research in the context of HMW-AGEs and cardiovascular dysfunction. However, the assessment of aortic fibrosis should be considered in future research. As already mentioned, LMW-AGEs increase collagen deposition between the endothelium and vascular smooth muscle, resulting in aortic stiffening. Aortic stiffening clinically manifests as hypertension and LV hypertrophy. Our research group has recently demonstrated signs of LV hypertrophy in rats injected with HMW-AGEs. Therefore, HMW-AGEs rats could also display aortic fibrosis, contributing to vascular dysfunction. This assessment should be combined with measuring the aortic AGEs content. Furthermore, we could elaborate more on the underlying mechanism of the HMW-AGEs-induced vasomotor imbalance. More specifically, endothelial production of vasodilators (*e.g.* NO and PGI_2) and vasoconstrictors (*e.g.* ET-1) requires further investigation. In addition, superoxide and peroxynitrite levels should be measured in aortic tissue to confirm the contribution of superoxide radical formation and oxidative stress. Finally, the acute effect of HMW-AGEs on vascular function, next to their chronic effect reported in this project, could be determined. In the long term, the results of this study support the development of new treatment strategies to improve cardiovascular outcome by targeting HMW-AGEs.

References

1. Maillard L. Action of amino acids on sugars. Formation of melanoidins in a methodical way. Compte-Rendu de l'Academie des Sciences. 1912;154:66-8.
2. Brownlee M, Cerami A, Vlassara H. Advanced glycosylation end products in tissue and the biochemical basis of diabetic complications. N Engl J Med. 1988;318(20):1315-21.
3. Singh R, Barden A, Mori T, Beilin L. Advanced glycation end-products: a review. Diabetologia. 2001;44(2):129-46.
4. Bunn HF, Higgins PJ. Reaction of monosaccharides with proteins: possible evolutionary significance. Science. 1981;213(4504):222-4.
5. Nishikawa T, Edelstein D, Du XL, Yamagishi S, Matsumura T, Kaneda Y, et al. Normalizing mitochondrial superoxide production blocks three pathways of hyperglycaemic damage. Nature. 2000;404(6779):787-90.
6. Thornalley PJ, Langborg A, Minhas HS. Formation of glyoxal, methylglyoxal and 3-deoxyglucosone in the glycation of proteins by glucose. Biochem J. 1999;344 Pt 1:109-16.
7. Goldberg T, Cai W, Peppa M, Dardaine V, Baliga BS, Uribarri J, et al. Advanced glycoxidation end products in commonly consumed foods. J Am Diet Assoc. 2004;104(8):1287-91.
8. Koschinsky T, He CJ, Mitsuhashi T, Bucala R, Liu C, Buenting C, et al. Orally absorbed reactive glycation products (glycotoxins): an environmental risk factor in diabetic nephropathy. Proc Natl Acad Sci U S A. 1997;94(12):6474-9.
9. Scheijen J, Hanssen NMJ, van Greevenbroek MM, Van der Kallen CJ, Feskens EJM, Stehouwer CDA, et al. Dietary intake of advanced glycation endproducts is associated with higher levels of advanced glycation endproducts in plasma and urine: The CODAM study. Clin Nutr. 2018;37(3):919-25.
10. Cerami C, Founds H, Nicholl I, Mitsuhashi T, Giordano D, Vanpatten S, et al. Tobacco smoke is a source of toxic reactive glycation products. Proc Natl Acad Sci U S A. 1997;94(25):13915-20.
11. Ulrich P, Cerami A. Protein glycation, diabetes, and aging. Recent Prog Horm Res. 2001;56:1-21.
12. Thornalley PJ, Battah S, Ahmed N, Karachalias N, Agalou S, Babaei-Jadidi R, et al. Quantitative screening of advanced glycation endproducts in cellular and extracellular proteins by tandem mass spectrometry. Biochem J. 2003;375(Pt 3):581-92.
13. Deluyker D, Evens L, Bito V. Advanced glycation end products (AGEs) and cardiovascular dysfunction: focus on high molecular weight AGEs. Amino Acids. 2017;49(9):1535-41.
14. Miura J, Yamagishi S, Uchigata Y, Takeuchi M, Yamamoto H, Makita Z, et al. Serum levels of non-carboxymethyllysine advanced glycation endproducts are correlated to severity of microvascular complications in patients with Type 1 diabetes. J Diabetes Complications. 2003;17(1):16-21.
15. Deluyker D, Ferferieva V, Noben JP, Swennen Q, Bronckaers A, Lambrichts I, et al. Cross-linking versus RAGE: How do high molecular weight advanced glycation products induce cardiac dysfunction? Int J Cardiol. 2016;210:100-8.
16. Aronson D. Cross-linking of glycated collagen in the pathogenesis of arterial and myocardial stiffening of aging and diabetes. J Hypertens. 2003;21(1):3-12.
17. Blackburn NJR, Vulesevic B, McNeill B, Cimenci CE, Ahmadi A, Gonzalez-Gomez M, et al. Methylglyoxal-derived advanced glycation end products contribute to negative cardiac remodeling and dysfunction post-myocardial infarction. Basic Res Cardiol. 2017;112(5):57.
18. Bidasee KR, Nallani K, Yu Y, Cocklin RR, Zhang Y, Wang M, et al. Chronic diabetes increases advanced glycation end products on cardiac ryanodine receptors/calcium-release channels. Diabetes. 2003;52(7):1825-36.
19. Bidasee KR, Zhang Y, Shao CH, Wang M, Patel KP, Dincer UD, et al. Diabetes increases formation of advanced glycation end products on Sarco(endo)plasmic reticulum Ca2+-ATPase. Diabetes. 2004;53(2):463-73.
20. Neeper M, Schmidt AM, Brett J, Yan SD, Wang F, Pan YC, et al. Cloning and expression of a cell surface receptor for advanced glycosylation end products of proteins. J Biol Chem. 1992;267(21):14998-5004.
21. Hudson BI, Carter AM, Harja E, Kalea AZ, Arriero M, Yang H, et al. Identification, classification, and expression of RAGE gene splice variants. Faseb j. 2008;22(5):1572-80.
22. Brett J, Schmidt AM, Yan SD, Zou YS, Weidman E, Pinsky D, et al. Survey of the distribution of a newly characterized receptor for advanced glycation end products in tissues. Am J Pathol. 1993;143(6):1699-712.
23. Ott C, Jacobs K, Haucke E, Navarrete Santos A, Grune T, Simm A. Role of advanced glycation end products in cellular signaling. Redox Biol. 2014;2:411-29.
24. Ren X, Ren L, Wei Q, Shao H, Chen L, Liu N. Advanced glycation end-products decreases expression of endothelial nitric oxide synthase through oxidative stress in human coronary artery endothelial cells. Cardiovasc Diabetol. 2017;16(1):52.

25. Yao D, Brownlee M. Hyperglycemia-induced reactive oxygen species increase expression of the receptor for advanced glycation end products (RAGE) and RAGE ligands. Diabetes. 2010;59(1):249-55.
26. Vlassara H, Fuh H, Makita Z, Krungkrai S, Cerami A, Bucala R. Exogenous advanced glycosylation end products induce complex vascular dysfunction in normal animals: a model for diabetic and aging complications. Proc Natl Acad Sci U S A. 1992;89(24):12043-7.
27. Tan KC, Chow WS, Ai VH, Metz C, Bucala R, Lam KS. Advanced glycation end products and endothelial dysfunction in type 2 diabetes. Diabetes Care. 2002;25(6):1055-9.
28. Lakatta EG, Levy D. Arterial and cardiac aging: major shareholders in cardiovascular disease enterprises: Part I: aging arteries: a "set up" for vascular disease. Circulation. 2003;107(1):139-46.
29. Schram MT, Henry RM, van Dijk RA, Kostense PJ, Dekker JM, Nijpels G, et al. Increased central artery stiffness in impaired glucose metabolism and type 2 diabetes: the Hoorn Study. Hypertension. 2004;43(2):176-81.
30. Sims TJ, Rasmussen LM, Oxlund H, Bailey AJ. The role of glycation cross-links in diabetic vascular stiffening. Diabetologia. 1996;39(8):946-51.
31. Yuan X, Zhang Z, Gong K, Zhao P, Qin J, Liu N. Inhibition of reactive oxygen species/extracellular signal-regulated kinases pathway by pioglitazone attenuates advanced glycation end products-induced proliferation of vascular smooth muscle cells in rats. Biol Pharm Bull. 2011;34(5):618-23.
32. Peeters SA, Engelen L, Buijs J, Theilade S, Rossing P, Schalkwijk CG, et al. Associations between advanced glycation endproducts and matrix metalloproteinases and its inhibitor in individuals with type 1 diabetes. J Diabetes Complications. 2018;32(3):325-9.
33. Laurent S, Boutouyrie P, Asmar R, Gautier I, Laloux B, Guize L, et al. Aortic stiffness is an independent predictor of all-cause and cardiovascular mortality in hypertensive patients. Hypertension. 2001;37(5):1236-41.
34. Bucala R, Tracey KJ, Cerami A. Advanced glycosylation products quench nitric oxide and mediate defective endothelium-dependent vasodilatation in experimental diabetes. J Clin Invest. 1991;87(2):432-8.
35. Wautier MP, Chappey O, Corda S, Stern DM, Schmidt AM, Wautier JL. Activation of NADPH oxidase by AGE links oxidant stress to altered gene expression via RAGE. Am J Physiol Endocrinol Metab. 2001;280(5):E685-94.
36. Ferrer-Sueta G, Campolo N, Trujillo M, Bartesaghi S, Carballal S, Romero N, et al. Biochemistry of Peroxynitrite and Protein Tyrosine Nitration. Chem Rev. 2018;118(3):1338-408.
37. Laursen JB, Somers M, Kurz S, McCann L, Warnholtz A, Freeman BA, et al. Endothelial regulation of vasomotion in apoE-deficient mice: implications for interactions between peroxynitrite and tetrahydrobiopterin. Circulation. 2001;103(9):1282-8.
38. Yamagishi S, Fujimori H, Yonekura H, Yamamoto Y, Yamamoto H. Advanced glycation endproducts inhibit prostacyclin production and induce plasminogen activator inhibitor-1 in human microvascular endothelial cells. Diabetologia. 1998;41(12):1435-41.
39. Adamopoulos C, Piperi C, Gargalionis AN, Dalagiorgou G, Spilioti E, Korkolopoulou P, et al. Advanced glycation end products upregulate lysyl oxidase and endothelin-1 in human aortic endothelial cells via parallel activation of ERK1/2-NF-kappaB and JNK-AP-1 signaling pathways. Cell Mol Life Sci. 2016;73(8):1685-98.
40. Zhang WJ, Li PX, Guo XH, Huang QB. Role of moesin, Src, and ROS in advanced glycation end product-induced vascular endothelial dysfunction. Microcirculation. 2017;24(3).
41. Stirban A, Gawlowski T, Roden M. Vascular effects of advanced glycation endproducts: Clinical effects and molecular mechanisms. Mol Metab. 2014;3(2):94-108.
42. Borg DJ, Forbes JM. Targeting advanced glycation with pharmaceutical agents: where are we now? Glycoconj J. 2016;33(4):653-70.
43. Brownlee M, Vlassara H, Kooney A, Ulrich P, Cerami A. Aminoguanidine prevents diabetes-induced arterial wall protein cross-linking. Science. 1986;232(4758):1629-32.
44. Corman B, Duriez M, Poitevin P, Heudes D, Bruneval P, Tedgui A, et al. Aminoguanidine prevents age-related arterial stiffening and cardiac hypertrophy. Proc Natl Acad Sci U S A. 1998;95(3):1301-6.
45. Thornalley PJ. Use of aminoguanidine (Pimagedine) to prevent the formation of advanced glycation endproducts. Arch Biochem Biophys. 2003;419(1):31-40.
46. Voziyan PA, Metz TO, Baynes JW, Hudson BG. A post-Amadori inhibitor pyridoxamine also inhibits chemical modification of proteins by scavenging carbonyl intermediates of carbohydrate and lipid degradation. J Biol Chem. 2002;277(5):3397-403.
47. Wu ET, Liang JT, Wu MS, Chang KC. Pyridoxamine prevents age-related aortic stiffening and vascular resistance in association with reduced collagen glycation. Exp Gerontol. 2011;46(6):482-8.

48. Deluyker D, Ferferieva V, Driesen RB, Verboven M, Lambrichts I, Bito V. Pyridoxamine improves survival and limits cardiac dysfunction after MI. Sci Rep. 2017;7(1):16010.
49. Engelen L, Stehouwer CD, Schalkwijk CG. Current therapeutic interventions in the glycation pathway: evidence from clinical studies. Diabetes Obes Metab. 2013;15(8):677-89.
50. Wolffenbuttel BH, Boulanger CM, Crijns FR, Huijberts MS, Poitevin P, Swennen GN, et al. Breakers of advanced glycation end products restore large artery properties in experimental diabetes. Proc Natl Acad Sci U S A. 1998;95(8):4630-4.
51. Vaitkevicius PV, Lane M, Spurgeon H, Ingram DK, Roth GS, Egan JJ, et al. A cross-link breaker has sustained effects on arterial and ventricular properties in older rhesus monkeys. Proc Natl Acad Sci U S A. 2001;98(3):1171-5.
52. Kass DA, Shapiro EP, Kawaguchi M, Capriotti AR, Scuteri A, deGroof RC, et al. Improved arterial compliance by a novel advanced glycation end-product crosslink breaker. Circulation. 2001;104(13):1464-70.
53. Zieman SJ, Melenovsky V, Clattenburg L, Corretti MC, Capriotti A, Gerstenblith G, et al. Advanced glycation endproduct crosslink breaker (alagebrium) improves endothelial function in patients with isolated systolic hypertension. J Hypertens. 2007;25(3):577-83.
54. Park L, Raman KG, Lee KJ, Lu Y, Ferran LJ, Jr., Chow WS, et al. Suppression of accelerated diabetic atherosclerosis by the soluble receptor for advanced glycation endproducts. Nat Med. 1998;4(9):1025-31.
55. Bucciarelli LG, Wendt T, Qu W, Lu Y, Lalla E, Rong LL, et al. RAGE blockade stabilizes established atherosclerosis in diabetic apolipoprotein E-null mice. Circulation. 2002;106(22):2827-35.
56. Liu Y, Yu M, Zhang L, Cao Q, Song Y, Liu Y, et al. Soluble receptor for advanced glycation end products mitigates vascular dysfunction in spontaneously hypertensive rats. Mol Cell Biochem. 2016;419(1-2):165-76.
57. Wautier JL, Zoukourian C, Chappey O, Wautier MP, Guillausseau PJ, Cao R, et al. Receptor-mediated endothelial cell dysfunction in diabetic vasculopathy. Soluble receptor for advanced glycation end products blocks hyperpermeability in diabetic rats. J Clin Invest. 1996;97(1):238-43.
58. Kajikawa M, Nakashima A, Fujimura N, Maruhashi T, Iwamoto Y, Iwamoto A, et al. Ratio of serum levels of AGEs to soluble form of RAGE is a predictor of endothelial function. Diabetes Care. 2015;38(1):119-25.
59. Kellow NJ, Savige GS. Dietary advanced glycation end-product restriction for the attenuation of insulin resistance, oxidative stress and endothelial dysfunction: a systematic review. Eur J Clin Nutr. 2013;67(3):239-48.
60. Di Pino A, Currenti W, Urbano F, Scicali R, Piro S, Purrello F, et al. High intake of dietary advanced glycation end-products is associated with increased arterial stiffness and inflammation in subjects with type 2 diabetes. Nutr Metab Cardiovasc Dis. 2017;27(11):978-84.
61. Macias-Cervantes MH, Rodriguez-Soto JM, Uribarri J, Diaz-Cisneros FJ, Cai W, Garay-Sevilla ME. Effect of an advanced glycation end product-restricted diet and exercise on metabolic parameters in adult overweight men. Nutrition. 2015;31(3):446-51.
62. Semba RD, Bandinelli S, Sun K, Guralnik JM, Ferrucci L. Relationship of an advanced glycation end product, plasma carboxymethyl-lysine, with slow walking speed in older adults: the InCHIANTI study. Eur J Appl Physiol. 2010;108(1):191-5.
63. Goon JA, Aini AH, Musalmah M, Anum MY, Nazaimoon WM, Ngah WZ. Effect of Tai Chi exercise on DNA damage, antioxidant enzymes, and oxidative stress in middle-age adults. J Phys Act Health. 2009;6(1):43-54.
64. Maessen MFH, Schalkwijk CG, Verheggen R, Aengevaeren VL, Hopman MTE, Eijsvogels TMH. A comparison of dicarbonyl stress and advanced glycation endproducts in lifelong endurance athletes vs. sedentary controls. J Sci Med Sport. 2017;20(10):921-6.
65. Delbin MA, Davel AP, Couto GK, de Araujo GG, Rossoni LV, Antunes E, et al. Interaction between advanced glycation end products formation and vascular responses in femoral and coronary arteries from exercised diabetic rats. PLoS One. 2012;7(12):e53318.
66. Schindelin J, Arganda-Carreras I, Frise E, Kaynig V, Longair M, Pietzsch T, et al. Fiji: an open-source platform for biological-image analysis. Nat Methods. 2012;9(7):676-82.
67. Sena CM, Matafome P, Crisostomo J, Rodrigues L, Fernandes R, Pereira P, et al. Methylglyoxal promotes oxidative stress and endothelial dysfunction. Pharmacol Res. 2012;65(5):497-506.
68. Grossin N, Auger F, Niquet-Leridon C, Durieux N, Montaigne D, Schmidt AM, et al. Dietary CML-enriched protein induces functional arterial aging in a RAGE-dependent manner in mice. Mol Nutr Food Res. 2015;59(5):927-38.
69. Candido R, Forbes JM, Thomas MC, Thallas V, Dean RG, Burns WC, et al. A breaker of advanced glycation end products attenuates diabetes-induced myocardial structural changes. Circ Res. 2003;92(7):785-92.
70. Furchgott RF, Zawadzki JV. The obligatory role of endothelial cells in the relaxation of arterial smooth muscle by acetylcholine. Nature. 1980;288(5789):373-6.

71. Palmer RM, Ferrige AG, Moncada S. Nitric oxide release accounts for the biological activity of endothelium-derived relaxing factor. Nature. 1987;327(6122):524-6.
72. Vallance P, Collier J, Moncada S. Effects of endothelium-derived nitric oxide on peripheral arteriolar tone in man. Lancet. 1989;2(8670):997-1000.
73. Goldin A, Beckman JA, Schmidt AM, Creager MA. Advanced glycation end products: sparking the development of diabetic vascular injury. Circulation. 2006;114(6):597-605.
74. Chen SX, Song T, Zhou SH, Liu YH, Wu SJ, Liu LY. Protective effects of ACE inhibitors on vascular endothelial dysfunction induced by exogenous advanced oxidation protein products in rats. Eur J Pharmacol. 2008;584(2-3):368-75.
75. Su Y, Mao N, Li M, Dong X, Lin FZ, Xu Y, et al. KB-R7943 restores endothelium-dependent relaxation induced by advanced glycosylation end products in rat aorta. J Diabetes Complications. 2013;27(1):6-10.
76. Eid BG, Abu-Sharib AT, El-Bassossy HM, Balamash K, Smirnov SV. Enhanced calcium entry via activation of NOX/PKC underlies increased vasoconstriction induced by methylglyoxal. Biochem Biophys Res Commun. 2018;506(4):1013-8.
77. Pieper GM, Gross GJ. Oxygen free radicals abolish endothelium-dependent relaxation in diabetic rat aorta. Am J Physiol. 1988;255(4 Pt 2):H825-33.
78. Zhang P, Li Y, Guo R, Zang W. Salidroside Protects Against Advanced Glycation End Products-Induced Vascular Endothelial Dysfunction. Med Sci Monit. 2018;24:2420-8.
79. Gryglewski RJ, Palmer RM, Moncada S. Superoxide anion is involved in the breakdown of endothelium-derived vascular relaxing factor. Nature. 1986;320(6061):454-6.
80. El-Bassossy HM, Neamatallah T, Balamash KS, Abushareb AT, Watson ML. Arginase overexpression and NADPH oxidase stimulation underlie impaired vasodilation induced by advanced glycation end products. Biochem Biophys Res Commun. 2018;499(4):992-7.
81. Mitchell JA, Kirkby NS. Eicosanoids, prostacyclin and cyclooxygenase in the cardiovascular system. Br J Pharmacol. 2019;176(8):1038-50.
82. Feng L, Xia Y, Garcia GE, Hwang D, Wilson CB. Involvement of reactive oxygen intermediates in cyclooxygenase-2 expression induced by interleukin-1, tumor necrosis factor-alpha, and lipopolysaccharide. J Clin Invest. 1995;95(4):1669-75.
83. Yang T, Zhang A, Pasumarthy A, Zhang L, Warnock Z, Schnermann JB. Nitric oxide stimulates COX-2 expression in cultured collecting duct cells through MAP kinases and superoxide but not cGMP. Am J Physiol Renal Physiol. 2006;291(4):F891-5.
84. Sarantitis I, Papanastasopoulos P, Manousi M, Baikoussis NG, Apostolakis E. The cytoskeleton of the cardiac muscle cell. Hellenic J Cardiol. 2012;53(5):367-79.
85. Sequeira V, Nijenkamp LL, Regan JA, van der Velden J. The physiological role of cardiac cytoskeleton and its alterations in heart failure. Biochim Biophys Acta. 2014;1838(2):700-22.
86. Bers DM. Cardiac excitation-contraction coupling. Nature. 2002;415(6868):198-205.
87. Diguet N, Mallat Y, Ladouce R, Clodic G, Prola A, Tritsch E, et al. Muscle creatine kinase deficiency triggers both actin depolymerization and desmin disorganization by advanced glycation end products in dilated cardiomyopathy. J Biol Chem. 2011;286(40):35007-19.
88. Milner DJ, Taffet GE, Wang X, Pham T, Tamura T, Hartley C, et al. The absence of desmin leads to cardiomyocyte hypertrophy and cardiac dilation with compromised systolic function. J Mol Cell Cardiol. 1999;31(11):2063-76.
89. Lemasters JJ. Selective mitochondrial autophagy, or mitophagy, as a targeted defense against oxidative stress, mitochondrial dysfunction, and aging. Rejuvenation Res. 2005;8(1):3-5.
90. Zha ZM, Wang JH, Li SL, Guo Y. Pitavastatin attenuates AGEs-induced mitophagy via inhibition of ROS generation in the mitochondria of cardiomyocytes. J Biomed Res. 2018;32(4):281-7.
91. Hou X, Hu Z, Xu H, Xu J, Zhang S, Zhong Y, et al. Advanced glycation endproducts trigger autophagy in cadiomyocyte via RAGE/PI3K/AKT/mTOR pathway. Cardiovasc Diabetol. 2014;13:78.
92. Hu P, Zhou H, Lu M, Dou L, Bo G, Wu J, et al. Autophagy Plays a Protective Role in Advanced Glycation End Product-Induced Apoptosis in Cardiomyocytes. Cell Physiol Biochem. 2015;37(2):697-706.
93. Jespersen B, Tykocki NR, Watts SW, Cobbett PJ. Measurement of smooth muscle function in the isolated tissue bath-applications to pharmacology research. J Vis Exp. 2015(95):52324.
94. Galan DT, Bito V, Claus P, Holemans P, Abi-Char J, Nagaraju CK, et al. Reduced mitochondrial respiration in the ischemic as well as in the remote nonischemic region in postmyocardial infarction remodeling. Am J Physiol Heart Circ Physiol. 2016;311(5):H1075-h90.
95. Lorenzi R, Andrades ME, Bortolin RC, Nagai R, Dal-Pizzol F, Moreira JC. Glycolaldehyde induces oxidative stress in the heart: a clue to diabetic cardiomyopathy? Cardiovasc Toxicol. 2010;10(4):244-9.

Curriculum vitae

EDUCATION AND WORK EXPERIENCE

Master Biomedical Sciences – Hasselt University, Diepenbeek, Belgium

2017 – now

- Senior practical training:
    - Master's thesis: 'High-molecular-weight advanced glycation end products disturb the vasomotor balance in rat aortic rings through superoxide formation.'
    - BIOMED – Biomedical Research Institute, Hasselt University, Diepenbeek, Belgium
    - Supervisor: Prof. dr. Virginie Bito
    - ***Abstract selected for oral presentation at MOSA Conference, Maastricht, Netherlands (26/06/2019)***
- Junior practical training:
    - Project: 'The effect of moderate intensity exercise on the progression of abdominal venous congestion in rats.'
    - BIOMED – Biomedical Research Institute, Hasselt University, Diepenbeek, Belgium
    - Supervisor: Prof. dr. Dominique Hansen

Bachelor Biomedical sciences – Hasselt University, Diepenbeek, Belgium

2014 - 2017

- Graduated with extinction
- Bachelor's thesis: 'The effect of abdominal venous congestion on cardiac expression and morphology in a new rat model for the cardiorenal syndrome'.
    - BIOMED – Biomedical Research Institute, Hasselt University, Diepenbeek, Belgium
    - Supervisor: Prof. dr. Quirine Swennen

SKILLS AND COMPETENCIES

- Research skills:
    - Western blot, PCR, histochemistry, ELISA, light and electron microscopy, blood sampling, echocardiography, hemodynamic assessment, cardiomyocyte isolation, cell shortening, patch clamp, research communication (oral and written)
- Additional courses:
    - Laboratory animal sciences (FELASA C certificate)
    - Cardiology course at Hasselt University
    - Oncology course at Hasselt University
    - Neuroscience course at Hasselt University
- Competencies:
    - Ambitious, passionate, curious, persevering, critical thinker, team player

SCIENTIFIC PUBLICATIONS

1. Cops J, **Haesen S***, De Moor B, Mullens W, Hansen D. Current animal models for the study of congestion in heart failure: an overview. 2019. Heart Failure Reviews (IF 4.104). *Equally contributing first author

2. Cops J, **Haesen S***, De Moor B, Mullens W, Hansen D. Is there a favorable effect of exercise intervention on congested organs in heart failure? Under review in Heart Failure Reviews (IF 4.104). *Equally contributing first author

3. Cops J, De Moor B, **Haesen S**, Lijnen L, Wens I, Lemoine L, et al. Endurance exercise intervention is beneficial to kidney function in a rat model of isolated abdominal venous congestion: a randomized controlled trial. Under review in Scientific Reports (IF 4.122).

4. Cops J, **Haesen S**, Lijnen L, Wens I, Lemoine L, De Moor B, et al. Moderate intense exercise as a new therapeutic strategy to tackle abdominal venous congestion in heart failure. Accepted congress abstract.

- EuroPrevent 2019 (Lisbon, Portugal)
- Belgian Society of Cardiology 2019 (Brussels, Belgium)